DEVELOPMENT OF STIFFNESS RELEASE MODEL FOR SIMULATING HIGH SPEED CRACK PROPAGATION IN PLATES

A Thesis Submitted

in Partial Fulfillment of the Requirements

for the Degree of

MASTER OF TECHNOLOGY

by

SAHANE DATTATRAYA G.

to the

DEPARTMENT OF MECHANICAL ENGINEERING

INDIAN INSTITUTE OF TECHNOLOGY, KANPUR

MARCH, 2003

CERTIFICATE

It is certified that the work contained in the thesis entitled **"Development of Stiffness Release Model for Simulating High Speed Crack Propagation in Plates"**, by *Sahane Dattatraya Ganpat*, has been carried out under my supervision and that this work has not been submitted elsewhere for a degree.

Dr. N. N. Kishore
(Professor)
Department of Mechanical Engg.
Indian Institute of Technology, Kanpur.

DEDICATED

TO

MY BELOVED PARENTS

ACKNOWLEDGEMENTS

I wish to express my deep sense of gratitude to my ever-cherished guide Dr. N.N. Kishore for his guidance, invaluable suggestions and constant encouragement. I am sincerely thankful for his valuable suggestions in my academic as well as personal life.

I wish to express my special thanks to Mr. Bhanu Kishore, Mr. Mukul Shukla, Mr. S. K. Rathore, for their invaluable suggestions and constant encouragement towards completion of my work.

I appreciate and extend my thanks to my lab mates Ramakrishna, Ashish and Samuel for their suggestions while I was developing the code.

I would like to thank all my IIT friends Hemant, Abhijit, Vidyanand, Sai, Manish and Mukesh for making my stay at IITK very enjoyable and memorable. I will cherish the moments forever.

Finally, I am grateful to the Almighty and my parents for what I am today.

Indian Institute of Technology, Kanpur.
March, 2003

-Sahane Dattatraya G.

ABSTRACT

The phenomenon of dynamic fracture is of interest in a wide variety of contexts from high-speed manufacturing and defence applications to geophysics and seismology. In dynamic fracture problems, role of material inertia becomes significant. The formulation and analytical solutions of dynamic fracture problems are very complex. Experimental and numerical methods like finite element method are used extensively for solving dynamic fracture problems. Existing methods for simulating crack phenomenon in dynamic fracture problems such as, moving mesh procedures or force release models, have certain drawbacks that they are either computationally very intensive or give oscillations in the solution.

Present work is a modification of 'Stiffness Release Model' [19, 20] developed for simulating high-speed dynamic crack propagation. In the 'Stiffness Release Model' the mesh is kept stationary and a 1-Dimensional elastic spring element is added at the crack tip node. The gradual propagation of the crack from one node to the next node is achieved by decreasing the stiffness value from a very large value (ideally infinite) to zero as the crack propagates to the next node within the element. But this model gives high oscillation at the element boundaries.

The emphasis of the present work is to improve the above 'Stiffness Release Model' by mass modification. Here mass of the element surrounding the crack tip is modified so that it varies as a function of non-dimensional crack length when crack extends through the element and the effect of other parameters with crack velocity is also studied which will enable in finding the propagation history under impact loading.

The finite element model is first validated for static case and then with hypothetical problem for different crack speeds. Results give smooth variation of energy release rate curve for different crack velocities.

CONTENTS

List of Figures

List of Symbols

a	Non-dimensional crack length
$a^{'}$	Semi crack length
A	Crack surface area
c	Dilation wave velocity
$\alpha^{'}, \delta^{'}$	Constants in Newmark's method of integration
α	Parameter in improved stiffness model
β	Parameter used in mass modification
C, C_1, C2	Constants in stiffness release model
C_0, K_1, K_2	Constants in stiffness release formulation
[D]	Elastic constitutive matrix
Det j	Determinant of Jacobian matrix
E	Young's modulus of elasticity
F_{HB}	Holding back force at the crack tip
{F}	Global force vector
G	Energy release rate
G_I	Energy release rate in mode 1
G_{II}	Energy release rate in mode 2
G_{III}	Energy release rate in mode 3
G_{crit}	Critical energy release rate
G_{ini}	Initiation toughness
G_{prop}	Propagation toughness
h	Thickness of the plate
γ_{xz}, γ_{yz}	Shear strains in X-Z and Y-Z planes respectively
K_I	Stress intensity factor in mode 1
K_{II}	Stress intensity factor in mode 2
K_{III}	Stress intensity factor in mode 3
K_s	Spring stiffness at the crack tip
K_0	Static crack stiffness at the crack tip
[K]	Global stiffness matrix

$[K]^{(e)}$	Elemental stiffness matrix
L	Length of the plate
[M]	Global mass matrix
$[M]^{(e)}$	Elemental mass matrix
M_x, M_y	Moments on faces perpendicular to X and Y axes due to σ_x and σ_y stresses respectively
M_{xy}	Twisting moment due to shear stress σ_{xy}
θ_x, θ_y	Midplane rotation of faces perpendicular to the X and Y-axes respectively
[N]	Matrix of interpolation function
N_θ, N_w, N_s	Shape function for θ, w, s variables
dt	Time step
pdur	Total pulse time
q	Amplitude of the load
$\{Q\}$	Displacement vector
$\{\dot{Q}\}$	Velocity vector
$\{\ddot{Q}\}$	Acceleration component
R	Crack resistance
S_x, S_y	Shear forces on faces perpendicular to the X and Y-axes respectively
$\{\sigma\}$	Stress component
$\{\varepsilon\}$	Strain Component
t_{at_max}	Rise time
T	Kinetic energy in the component
L, ∇	Operators
ρ	Mass density of the plate
U	Strain energy in the component
u_0	Displacement of the node when crack tip reaches to the end of next element
u, v, w	Displacement components
V	Crack velocity

W_{ext}	Work done due to external forces
Π	Total potential energy
W	Width of the plate
ν	Poisson's ratio

CHAPTER 1

INTRODUCTION

1.1 Introduction

The phenomenon of dynamic fracture is of interest in a wide variety of contexts from high-speed manufacturing and defence applications to geophysics and seismology. A considerable amount of research has been directed towards the solution of problems involving the interactions of stress waves with cracks and boundaries to improve understanding of the behaviour of material failure under dynamic loading. The study of crack interaction is also of great interest from the point of view of quantitative non-destructive evaluation of structural materials.

The dynamic fracture phenomenon can be characterised by various dynamic states of crack tip. The dynamic states of crack tip are induced by impact loading applied to the cracked solids, or by fast motions of the crack tip itself. Dynamic loads may be created by moving vehicles, wind, gusts, shocks or blasts, unbalanced machines, wave impacts, seismic disturbances, etc. For solving these problems, often the time variation is neglected and they are treated as static or quasi-static problems. Structural members, which are subjected to cyclic loading such as vibrations, microscopic imperfections in the material give rise to microscopic cracks which in turn grow into cracks of significant size over passage of time. At this stage, further growth of cracks stably or unstably leading to the component failure depends not only on the material characteristics but also on the nature of loading, i.e., static or dynamic. For many dynamic problems, it is impossible to find closed form solutions, especially if they involve the aspect of fracture. A number of analytical solutions to problems of dynamic fracture shedding important light on the basic phenomenon have been reported in the past two decades. These solutions are however limited to simple cases of loading and of unbounded plane bodies. Usually, the interactions of the stress waves emanating from

the crack tip and those reflected from the boundaries of a finite body make the analytical solutions invalid. Thus, it often becomes mandatory to analyse dynamic crack propagation in finite solids using numerical methods.

1.2 Dynamic Fracture Mechanics

Dynamic fracture mechanics is the subfield of fracture mechanics concerned with fracture phenomena for which the role of material inertia becomes significant. One method of classifying dynamic fracture problems is as follows (Nishoka and Atulri, 1986, [1]):

(1) Solids containing stationary cracks subjected to dynamic loading.

(2) Solids containing dynamically propagating cracks under quasi-static loading.

(3) Solids containing dynamically propagating cracks under dynamic loading.

A knowledge of time-dependent asymptotic stress and displacement fields near the crack tip, and their "strength" as quantified, for instance, by the "stress intensity factor (SIF) in linearly elasto-dynamics, is basic in understanding the process and nature of dynamic fracture in solids. A direct approach to laboratory evaluation of dynamic fracture toughness and crack arrest toughness, is based on the laboratory measurements of the instruments dynamic stress fields close to the propagating crack tip using photo-elastic method. Such direct measurements, however, are generally difficult. To overcome these difficulties, and simplify the measurements necessary, hybrid experimental-numerical methods are often preferred. This is one reason that the advancement of the state of science of dynamic fracture mechanics relies heavily on simultaneous advances in computational methods.

Dynamic fracture mechanics concerns (i) the onset of crack growth under dynamic loading (ii) dynamic crack propagation in stressed solids. The conventional linear elasto-plastic or quasi-static fracture mechanics applies only up to the end of stable growth under quasi-static loading and assumes that the onset of unstable crack

propagation renders the structure useless. Yet, the prevention of crack growth initiation itself may be too conservative or too costly an objective for some structural designs, and also catastrophic failures caused by unstable crack growth are obviously intolerable. In these cases, the assurance of crack arrest, as a second line of defence, is essential. This concept has been investigated for design methodologies assuring the integrity of nuclear pressure vessels under thermal shock conditions, LNG ship hulls, and gas transmission pipelines.

The fundamental frame work of the subject of dynamic fracture mechanics, relies primarily on solutions for dynamic behaviour of solid containing cracks these solutions are characterized by, (i) stress wave integration (ii) the need to account for kinetic energy in the global energy balance of the fracturing body, and (iii) inertia effects of the material. The inertia effect may arise due to two reasons (i) rapidly applied load on a cracked solid and (ii) rapid crack propagation. In the first case the influence of the load is transferred to the crack by stress waves through the material. In the second case, the material particles on the two crack faces displace with respect to each other, as the crack advances. In the first case, inertia effect will be significant if the characteristic time (i.e. maximum load by the rate of load increase) is larger than time required for stress wave to travel at the characteristic wave speed of the material over a representative length of the body (crack length or distance from crack edge to the loaded boundary) (Freund, 1990, [2]). In the second case, the inertia effect should be accounted for whenever the crack velocity is a significant fraction of the characteristic wave speed of the material.

In the past two decades or so, a number of analytical solutions, which provide a useful understanding of dynamic crack behaviour, have been obtained. These analytical solutions are however, limited to cases of simple loading and unbounded plane bodies. Moreover, the stress wave introductions, which play an important role in dynamic fracture mechanics, usually render the analytical solutions intractable.

Therefore, the use of numerical methods is often indispensable for the analysis of cracks in finite solids.

The finite element method was more suitable for the analysis of stationary cracks under dynamic loading, due to the fact that the relevant singularities can be modelled in the crack tip elements. In large measure, this is the result of the development of finite element procedures to model propagating singularities and of path-independent integrals that characterize the strength of the fields near propagating crack tips.

1.3 Energy Concepts in dynamic fracture mechanics

Analytical methods based on the work done by applied loads and the changes in the energy of a system that accompany a real or virtual crack advance have been of central importance in the development of dynamic fracture mechanics. Griffith (1920, [3]) recognized the importance of the variation of the energy measures during crack growth. Consequently, for an elastic body containing a crack, the negative of the rate of change of total potential energy with respect to crack dimension is called the 'Energy Release Rate', G and is a function of crack size in general. G is the amount of energy, per unit length along the crack edge that is supplied by the elastic energy in the body and by the loading system in creating the new fracture surface.

1.3.1 Dynamic Energy Release Rate

The dynamic energy release rate is defined as the rate of mechanical energy flow out of the body and into the crack tip per unit crack advance. The energy flux, or energy flow per unit time, must be divided by v, the crack movement per unit time, in order to obtain the energy release from the body per unit crack advance. For two-dimensional fields, G is the mechanical energy released per unit thickness of the body in the direction perpendicular to the plane of deformation.

1.4 Rapid (Fast) Crack Propagation

Analyses of fast crack growth in structural mechanics have generally been based on an approach where a material and crack speed dependent value of a characterizing parameter, such as the energy release rate or the stress intensity factor, is used in conjunction with a crack tip equation of motion, Freund(1990,[2]).

1.4.1 Fast crack growth at constant speed

The assumption of constant speed results in significant simplification of the boundary value problem to be solved for the governing partial differential equations. The restriction to the constant speed crack growth permits a reduction of the number of independent variables by one and the analysis is simplified considerably. But some of the features of the crack growth process that are physically significant are overlooked in this approach.

1.4.2 Crack growth at nonuniform speed

The assumption of constant speed growth is imposed in order to render the mathematical models tractable. The study of a problem involving crack growth at nonuniform speed proceeds in two steps

1) The boundary value problem is considered for arbitrary motion of the crack tip, with a view toward obtaining a full description of the mechanical fields near the crack edge during growth.
2) An addition physical postulate in the form of a crack propagation criterion is imposed on the mechanical fields in order to determine an equation of motion for crack tip. The analytical approaches developed for stationary cracks and cracks growing at a constant speed can't extend to the case of nonuniform crack growth.

1.5 Fracture Model for dynamic crack propagation

Over the last few years, physicists interested in nonlinear phenomena have returned to problems of crack propagation, and to the study of model problems in which cracks develop from the breaking of bonds. Also, it is now possible to model the entire development of a crack, in a finite-element model of a continuum, even with inelastic effects (that is, plasticity) allowed for. Damage mechanics is well developed at the phenomenological level, and can also be built into codes that predict fracture. The admission of any model for microscopic processes introduces a length scale, and size effects may emerge. These are of practical importance as well as theoretical interest. Mathematical theory based on variational methods is developing, at least for cracks in elastic media. However, many problems remain: there is no adequate theory for the stability of a propagating crack, even in the framework of linear elasticity, at the present time. Interactions between macro- and micro-cracks require better modelling. The development of (approximate) fractal structure has so far not been modelled mechanistically. Some hint of the influence of underlying lattice structure has been demonstrated (it may apparently prevent steady-state propagation at low speed) but this is not fully worked out.

1.6 Literature Survey

Though considerable amount of work has been done to study the fracture phenomena through numerical methods, only rectangular double cantilever beam (DCB) specimens were given special interest. Owen and Shantaram (1977, [4]) started the case of finite element method to study dynamic crack growth. They studied DCB specimen and pipeline problem under transient loading. The crack was advanced from one node to the next node and when stress at the gauss point nearest to the crack tip

exceeded a certain value, damping coefficient was made zero at the released node. The crack propagation history was simulated for the given loading conditions.

Nishioka and Atluri (1982b, [5]) investigated the crack propagation and arrest in high strength steel DCB specimen using moving singular dynamic finite element procedure. An edge crack in a rectangular DCB specimen was propagated by inserting a wedge and the results were compared with experimental data. In another work, Nishioka and Atluri (1982a, [6]) presented the results of generation and prediction studies of dynamic crack propagation in plane stress and plane strain cases. The studies were conducted by using FEM, taking into account stress singularity near the crack tip. Variation of dynamic stress intensity factor with time and variation of dynamic fracture toughness with velocity were studied and compared with available experimental results.

Nishioka and Atluri (1986, [1]) gave elaborate information on the analysis of dynamic fracture using FEM. The most common way to deal with the crack tip region was to simulate crack growth through gradual release of elemental nodal forces or embedding a moving element in which interpolation functions are determined by the continuum near tip fields at the crack tip in the mesh, and J-Integral consideration. Following special description the differential equation in time for the node point variables must be integrated. Because the dynamic fields associated with rapid crack growth are rich in high frequency content, small time steps are required for accuracy. Because of natural restriction to small time steps, the author's report that many times combination of conditionally stable explicit time integration scheme and diagonalised mass matrix are found to be accurate.

Chiang (1990, [7]) presented a numerical procedure based on eigen function to determine the dynamic stress intensity factor for a crack moving at steady state under antiplane strain condition. An edge crack problem and a radial crack problem were solved using traction and displacement boundary conditions separately. It was shown that the dynamic effect was relatively insignificant for low crack propagation speeds provided that specimen size was fairly large.

Thesken and Gudmundson (1991, [8]) worked with elasto-dynamic moving element formulation incorporating a variable order singular element to enhance the local crack tip description. Kennedy and Kim (1993, [9]) incorporated micropolar elasticity theory into a plane strain finite element formulation to analyse the dynamic response of the crack. Materials with strong micropolar properties were found to have significantly lower dynamic energy release rate than their classical material counterparts.

Wang and Williams (1994, [10]) investigated high-speed crack growth in a thin double cantilever beam specimen using FEM. The cantilever end was loaded under an initial step displacement of 1mm and then pulled with a constant velocity the crack was propagated at assumed speed by gradual node release technique. Large dynamic effects were observed because of wave reflections within finite specimen size. The reflection and interaction of the waves from free boundary were avoided by limiting the duration of study. Chandra and Krauthammer (1995, [11]) investigated effects of rapidly applied load on the J-integral and stress intensity factor (K) of a cracked solid. Variation of J has been studied using energy balance approach, whereas that of K has been dealt with elastodynamic considerations together with several simplifying assumptions and approximations. Lee, Hawong and Choi (1996, [12]) studied propagating crack problems of orthotropic material under the dynamic plane mode. Dynamic stress components and dynamic displacement components around the crack tip of an orthotropic material under the dynamic load and the steady state in crack propagation were derived. When the crack propagation speed approaches zero, dynamic stress components and dynamic displacement components are identical to those of static state. The stress component values of the crack tip are greater when the fiber direction coincides with the direction of the stress component than when the fiber direction is normal to the stress component.

Lin and Smith (1997, [13]) presented a method wherein crack growth is predicted in a step by step basis from Paris law using stress intensity factor calculated by using finite element method. The crack front is defined by a cubic spline curve

from a set of nodes. Both the one quarter node crack opening and 3-D J-Integral method are used to calculate stress intensity factor. Automatic remeshing of finite element model to a new position that defines the new crack front enables the crack propagation to be followed. Beissel, Johnson and Popelar (1998, [14]) presented an algorithm, which allows crack propagation in any direction but doesn't require remeshing or the definition of new contact surfaces. This is achieved by tracking the path of the crack tip and failing the element crossed by the path such that they can no longer sustain tensile volumetric stress. The edges of these failed elements simulate crack faces that can sustain only compressive normal traction.

Zhuang and Guo (1999, [15]) addressed recent developments in the area of dynamic fracture mechanics and the applications of analysis methods to the rapid crack propagation for gas pipelines. Criteria for crack initiation, propagation and arrest were discussed. Christina and Christer (2001, [16]) presented a method for obtaining the complex stress intensity factor for an interface crack in a bimaterial using minimum number of computations. A crack closure integral method has been used. Falk, Needleman and Rice (2001, [17]) performed simulation on a square block in plain strain with an initial edge crack loaded at a constant rate of strain.

Brener and Spatschek (2002, [18]) presented a continuum theory which describes the fast growth of a crack by surface diffusion. It predicts the saturation of steady state crack velocity appreciably below the Rayleigh speed and tip blunting.

1.4 Present Work

Present work is a modification of 'Stiffness Release Model' [19, 20] developed for simulating high-speed dynamic crack propagation. In the 'Stiffness Release Model' developed by Kishore, Reddy and Deshmukh [19,20], the mesh is kept stationary and a 1-Dimensional elastic spring element is added at the crack tip node. The gradual propagation of the crack from one node to the next node is achieved by decreasing the stiffness value from a very large value (ideally infinite) to zero as the crack propagates to the next node within the element. But this model gives high oscillation at the element boundaries.

The emphasis of the present work is to improve the above stiffness Release Model by mass modification. Here mass of the element surrounding the crack tip is modified so that it varies as a function of non-dimensional crack length when crack extends through the element and the effect of other parameters with crack velocity is also studied which will enable in finding the propagation history under impact loading.

Chapter 2 describes the basics of FEM formulation and the existing propagation model.

Chapter 3 presents the crack propagation element model.

Chapter 4 describes the results and discussion.

Chapter 5 presents the conclusion of the present work and scope of future work.

CHAPTER 2

FEM FORMULATION AND CRACK MODELING

2.1 Basics of Dynamic Analysis of Plates with Crack

Plates with cracks subjected to dynamic load is solved using the theory of flexural motion of plates developed by Mindlin (1951, [21]) in which the three physical boundary conditions, viz. applied bending moments, twisting moment and transverse shear can be satisfied independently at the crack edge, whereas, the approximate Kirchhoff method can satisfy only two boundary conditions on the crack face leading to unrealistic results.

2.1.1 Mindlin Plate Theory

Consider the plate shown in Figure 2.1. The X and Y-axes are defined to be in the mid plane of the plate and z-axis is normal to the plane of the plate. The corresponding displacement components are u, v and w, respectively. Making the following assumptions:

1) The strains and stresses in the Z direction are negligible

2) The normal to the middle plane of the plate remains straight during deformation

static equilibrium equations for the plate bending problem can be obtained (Zienkiewicz, 1991, [22]; Timoshenko, (1959, [23]) in terms of mid plane rotations (θ_x, θ_y), lateral displacement (w) of the mid plane and shear force (S) at the mid plane. The representations of variables used in plate approximation are shown in Figure 2.2.

For dynamic analysis inertia effects have to be considered. Using D'Alemberts principle of motion, forces due to mass and moment of inertia, are taken into account in the equilibrium equations. With reference to the convention shown in Figure 2.2 the final equations are modified as follows (Mindlin, 1951, [21]):

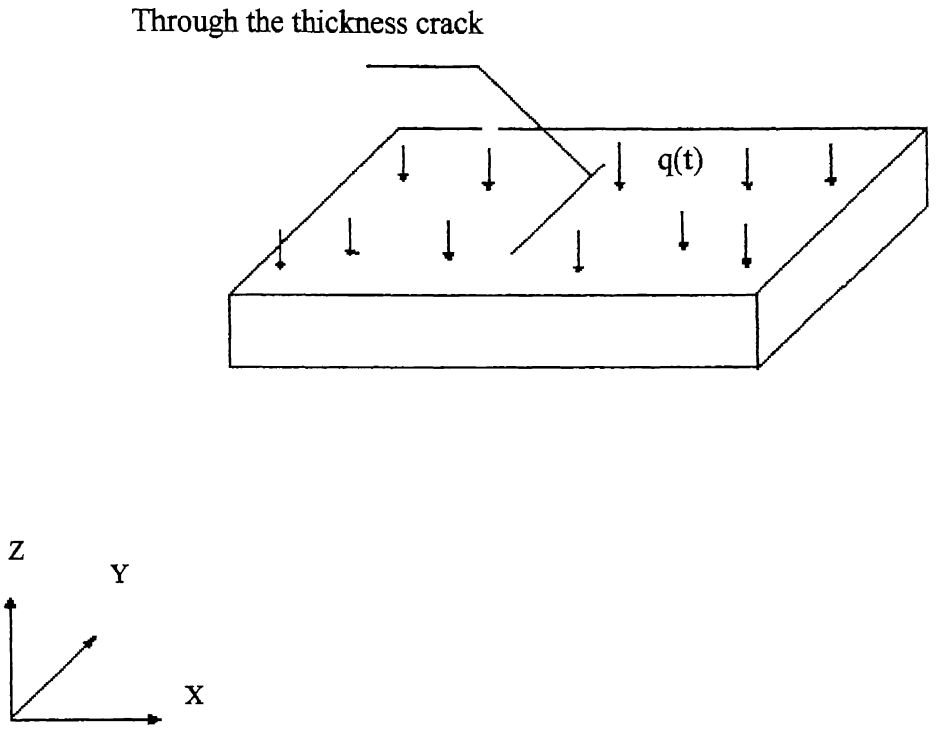

Figure 2.1 Cracked plate subjected to lateral dynamic load

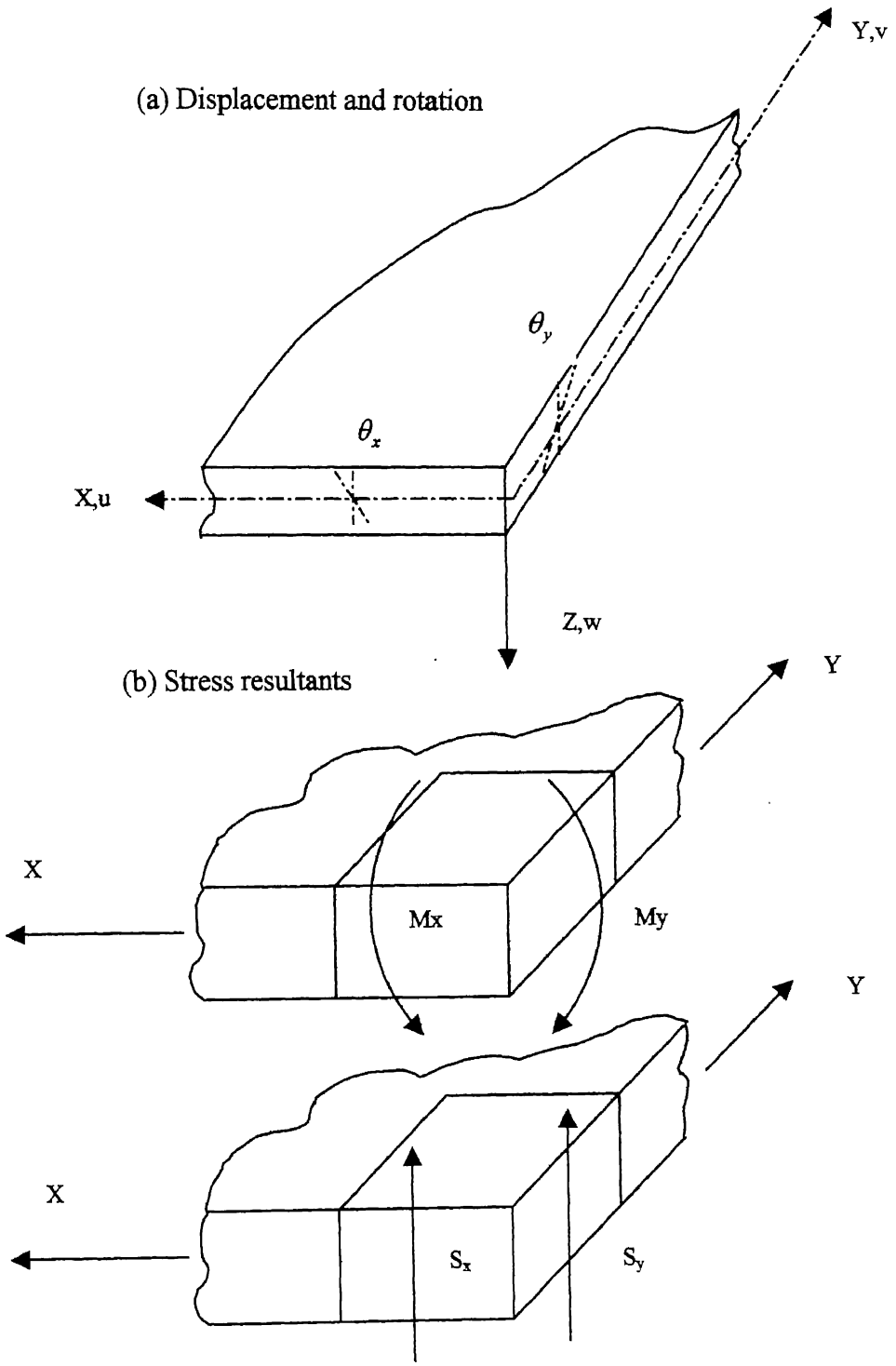

Figure 2.2 Variables For Plates

$$\frac{\partial M_x}{\partial x}+\frac{\partial M_{xy}}{\partial y}+S_x-\frac{\rho h^3}{12}\ddot{\theta}_x=0$$

$$\frac{\partial M_{xy}}{\partial x}+\frac{\partial M_y}{\partial y}+S_y-\frac{\rho h^3}{12}\ddot{\theta}_y=0 \qquad (2.1)$$

$$\frac{\partial S_x}{\partial x}+\frac{\partial S_y}{\partial y}+q-\rho h\ddot{w}=0$$

where,

$$-\theta x+\frac{\partial w}{\partial x}=\frac{1}{Gh}S_x \qquad (2.2)$$

and

$$-\theta y+\frac{\partial w}{\partial y}=\frac{1}{Gh}S_y$$

$$M_x=\int_{-h/2}^{h/2}\sigma_x\, z\, dz,$$

$$M_y=\int_{-h/2}^{h/2}\sigma_y\, z\, dz, \qquad (2.3)$$

$$M_{xy}=\int_{-h/2}^{h/2}\sigma_{xy}\, z\ dz,$$

$$\varepsilon_x=z\frac{\partial\theta_x}{\partial x}$$

$$\varepsilon_y=z\frac{\partial\theta_y}{\partial y} \qquad (2.4)$$

$$\gamma_{xz}=-\theta_x+\frac{\partial w}{\partial x}$$

$$\gamma_{yz}=-\theta_y+\frac{\partial w}{\partial y} \qquad (2.5)$$

where,

ρ is the mass density of the plate,

M_x and M_y are moments on faces perpendicular to X and Y axes due to σ_x and σ_y stresses respectively,

M_{xy} is the twisting moment due to shear stress σ_{xy},

θ_x and θ_y are the rotation of faces perpendicular to the X and Y-axes respectively,

S_x and S_y are shear forces on faces perpendicular to the X and Y-axes respectively,

ε_x and ε_y are strains along X and Y-axes respectively, and

γ_{xz} and γ_{yz} are shear strains in X-Z and Y-Z planes respectively.

2.2 Finite Element Formulation

2.2.1 FEM Equation

The problem is formulated in the three sets of variables θ, S and w, which are expressed in terms of nodal parameters using appropriate shape functions and parameters as

$$\theta = \begin{bmatrix} \theta_x \\ \theta_y \end{bmatrix} = N_\theta \bar{\theta}$$

$$S = \begin{bmatrix} S_x \\ S_y \end{bmatrix} = N_S \bar{S} \tag{2.6}$$

$$w = N_w \bar{w}$$

where N_θ, N_S and N_w are the shape function and $\bar{\theta}$, $\bar{S}$ and $\bar{w}$ are the nodal variables.

Using the notation of Eqn. (2.6) ,Eqn. (2.1) can be rewritten in the matrix form as

$$L^T D L\theta + S - \frac{\rho h^3}{12}\ddot{\theta} = 0$$

$$-\theta - C_1 S + \nabla w = 0 \tag{2.7}$$

$$\nabla^T S + q - \rho h \ddot{w} = 0$$

where L, ∇ are operators, C_1 is matrix,

$$L=\begin{bmatrix}\frac{\partial}{\partial x} & 0\\ 0 & \frac{\partial}{\partial y}\\ \frac{\partial}{\partial y} & \frac{\partial}{\partial x}\end{bmatrix} \qquad \nabla=\begin{bmatrix}\frac{\partial}{\partial x}\\ \frac{\partial}{\partial y}\end{bmatrix} \qquad C_1=\frac{1}{Gh}\begin{bmatrix}1 & 0\\ 0 & 1\end{bmatrix} \tag{2.8}$$

and D is property matrix as

$$D=\frac{Eh^3}{12(1-\nu^2)}\begin{bmatrix}1 & \nu & 0\\ \nu & 1 & 0\\ 0 & 0 & \frac{(1-\nu)}{2}\end{bmatrix}$$

Now, using Galerkin method of deriving FEM equations with weighting functions N_θ^T, N_S^T, N_w^T on Equation 2.7 and integrating over the domain of the problem, Ω, the following equations are obtained (Zienkiewcz, 1991, [22])

$$\begin{aligned} &A\bar{\theta}+B\bar{S}+E\ddot{\bar{\theta}}=f_\theta\\ &B^T\bar{\theta}-P\bar{S}+C\bar{w}=0\\ &C^T\bar{S}+F\ddot{\bar{w}}=f_w \end{aligned} \tag{2.9}$$

where

$$\begin{aligned} A&=\int_\Omega (LN_\theta)DLN_\theta^T d\Omega\\ B&=-\int_\Omega N_\theta^T N_S d\Omega\\ C&=\int_\Omega N_S^T(\nabla N_w)d\Omega\\ P&=-\int_\Omega N_S^T C_1 N_S d\Omega\\ f_\theta&=\int_\Gamma N_\theta^T T d\Gamma\\ f_w&=\int_\Omega N_w^T q d\Omega\\ E&=\frac{\rho h^3}{12}\int_\Omega N_\theta^T N_\theta d\Omega \end{aligned} \tag{2.10}$$

$$F = \rho h \int_{\Omega} N_w{}^T N_w d\Omega$$

Here, the vector T represents the two moment components imposed on the boundary by the traction and F represents the imposed shear force. The shape functions N_θ and N_w are chosen to have C_0 continuity but N_S can be discontinuous between elements.

Indeed, such a choice allows $\bar{S}$ to be locally defined for each element and thus be eliminated at element level when P≠0 and the main problem includes only the variables $\bar{\theta}$ and $\bar{w}$ which have inertia components.

Thus, equation (2.9) can be simplified by eliminating $\bar{S}$ (using the second equation) in terms of $\bar{\theta}$ and $\bar{w}$, as:

$$\begin{bmatrix} A+BP^{-1}B^T & BP^{-1}C \\ C^TP^{-1}B^T & C^TP^{-1}C \end{bmatrix} \begin{bmatrix} \bar{\theta} \\ \bar{w} \end{bmatrix} + \begin{bmatrix} E & 0 \\ 0 & F \end{bmatrix} \begin{bmatrix} \ddot{\bar{\theta}} \\ \ddot{\bar{w}} \end{bmatrix} = \begin{bmatrix} f_\theta \\ f_w \end{bmatrix} \qquad (2.10)$$

in general this equation will be referred as ,

$$[K]^e\{Q\} + [M]^e\{\ddot{Q}\} = \{F\}^e \qquad (2.11)$$

Such element equations are assembled to form the global equations as

$$(\Sigma[K]^e)\{Q\} + (\Sigma[M]^e)\{\ddot{Q}\} = \Sigma\{F\}^e$$

The final set of assembled equations can be written as,

$$[K]\{Q\} + [M]\{\ddot{Q}\} = \{F\} \qquad (2.12)$$

where

$[M] = \sum [M]^e$, Global mass matrix

$[K] = \sum [K]^e$, Global stiffness matrix

$\{F\} = \sum \{F\}^e$, Global applied force vector

and $[K]^{(e)}$, $[M]^{(e)}$ and $\{F\}^{(e)}$ are Elemental Stiffness Matrix, Elemental Mass Matrix and Elemental Force Vector.

2.2.2 Integration Algorithm

Eqn. (2.12) represent a system of linear differential equation of second order and the solution to the equation can be obtained by standard procedures of solving differential equations. The

procedures for solving differential equations are divided into direct integration and mode superposition of which former are preferred in wave propagation problem. In direct integration scheme, there are many different methods, which can be classified as 'Explicit' or 'Implicit' whose advantages and disadvantages are given by (Bathe, 1990, [24]).

In the present work, Newmark's method of integration is used.

Newmark's method is an extension of 'Linear acceleration method', in which, linear variation of acceleration is assumed from time t to $t+\Delta t$.

Velocity and acceleration approximated in terms of displacements are

$$^{t+\Delta t}\{\dot{q}\} = {}^{t}\{\dot{q}\} + \left[(1-\delta'){}^{t}\{\ddot{q}\} + \delta'^{\,t+\Delta t}\{\ddot{q}\}\right]\Delta t \tag{2.13}$$

$$^{t+\Delta t}\{q\} = {}^{t}\{q\} + {}^{t}\{\dot{q}\}\Delta t + \left[\left(\frac{1}{2}-\alpha'\right){}^{t}\{\ddot{q}\} + \delta'^{\,t+\Delta t}\{\ddot{q}\}\right]\Delta t^2 \tag{2.14}$$

where α' and δ' are the parameters chosen have accuracy and stability.

Usually, α' and δ' are taken as 0.25 and 0.5 respectively to get unconditional stability

2.3 Energy Release Rate and Its Determination

In fracture mechanics a crack can be characterized by four different parameters

i. Energy release rate (G_I, G_{II}, G_{III}) is energy based and is applied to brittle and less ductile material
ii. Stress intensity factor (K_I, K_{II}, K_{III}) is stress based. This parameter is applied to brittle and less ductile material.
iii. J-Integral (J), which has been developed to deal with ductile material and can also be applied to brittle material as well.
iv. Crack tip opening displacement (CTOD) is displacement based and is developed for ductile materials.

From computational point of view, stress intensity factor require special element so as to simulate stress singularity at the crack tip whereas J-Integral and energy release do not require any such modeling of stress singularity. In energy release rate approach, energy is

found out in entire domain and in J-Integral, evaluation is done along a path far away from crack tip. Thus both these approaches cleverly avoid analysis close to the crack tip and don't need any modeling of stress singularity.

Griffith (1920, [3]) outlined that in brittle fracture, as the crack extends new surfaces are formed. Formation of new surface requires surface energy. Consequently, crack in a brittle solid should advance when the reduction of the total potential energy of the body during a small amount of crack advance equals the surface energy of the new surface thereby created. Most of the energy release, as the crack advances, comes from the parts of the component, which are adjacent to the cracked surface. Two important parameters need to be considered

1) How much energy is released when a crack advances

2) Minimum energy required for crack to advance in forming two new surfaces.

First parameter is measured in terms of energy release rate denoted by G. G is a function of crack size in general. Thus the energy release rate is defined as energy release per unit area extension of crack growth if there is a virtual crack growth, i.e. energy equal to G would be released from the system per unit extension of area. This energy is supplied by the elastic energy in the body and by the loading system.

The energy requirement for a crack to grow per unit area extension is called as crack resistance and is usually denoted by symbol R. Crack resistance is sum of energy required to:

1) Form new surface

2) Cause anelastic deformation

Both the available energy release rate and crack resistance are important to study the possibility of crack becoming critical. Obviously, when the available energy release rate far exceeds the crack resistance, the crack starts to grow at high speed. In the present study 'energy release rate' is adopted, as it is a more comprehensive concept.

As the crack advances,

1) Stiffness of the component decreases.

2) Strain energy in the component either increases or decreases.

3) Work is done on the component if there is an application of load.

4) Energy is being consumed to create two new surfaces.

Formulation for energy release rate is carried out invoking the principle of conservation of energy. First, consider thesis quasi-static crack growth case. Let the incremental increase in the crack area be ΔA. This crack growth is achieved by an incremental external work done by the external forces and the strain energy within the body of the component increases

Let the incremental work by external force be ΔW_{ext}, change in strain energy be ΔU, and the available energy, GΔA, satisfy energy balance equation as follows:

$$G\Delta A = \Delta W_{ext} - \Delta U \tag{2.15}$$

$$G = -\frac{d}{dA}(U - W_{ext}) \tag{2.16}$$

$$G = -\frac{d\Pi}{dA} \tag{2.17}$$

where Π is the potential energy

For a plate of uniform thickness B, dA= Bda

where da is the incremental crack length, B is the thickness of the plate

$$G = -\frac{1}{B}\frac{d\Pi}{da} \tag{2.18}$$

For dynamic crack propagation problem, the kinetic energy, T, of the body should be taken into consideration. Dynamic energy release rate, G_D, is different as some energy may be consumed to impart kinetic energy to the cracked portion of the body and to generate stress waves.

For dynamic case, energy balance becomes

$$G\Delta A = \Delta W_{ext} - \Delta U - \Delta T \tag{2.19}$$

where ΔT is the increment in kinetic energy in the body.

For constant velocity crack propagation,

$$G = \frac{1}{B}\frac{d}{da}(W_{ext} - U - T) \tag{2.20}$$

For crack moving with velocity v,

$$G = \frac{1}{B}\frac{\frac{d}{dt}(W_{ext} - U - T)}{v} \tag{2.21}$$

In the present study, energy release rate is found out using equation (2.19).Different energies are found out using

$$W_{ext} = \{Q\}^T \{F\} \tag{2.22}$$

$$[U] = \frac{1}{2}\{Q\}^T [K]\{Q\} \tag{2.23}$$

$$T = \frac{1}{2}\{\dot{Q}\}^T [M]\{\dot{Q}\} \tag{2.24}$$

where,

W_{ext} is the external work done

U is the strain energy in the component

T is the kinetic energy in the component

$\{F\}$ is the external force vector

$\{Q\}$ is the displacement vector

$\{\dot{Q}\}$ is the velocity vector

$[K]$ is the global stiffness matrix

[M] is the global mass matrix

2.4 Closure

In this chapter, formulation of FEM equation is described along with integration algorithms for solving equilibrium equation governing linear dynamic response of a system of finite element, which will be used in the next chapters to construct a propagation element. This chapter also describes some general concepts in energy and energy release rate.

CHAPTER 3

CRACK PROPAGATION ANALYSIS

3.1 Introduction

Over the last few years, physicists interested in nonlinear phenomena have returned to problems of crack propagation, and to the study of model problems in which cracks develop from the breaking of bonds. Also, it is now possible to model the entire development of a crack, in a finite-element model of a continuum, even with inelastic effects (that is, plasticity) allowed for. Damage mechanics is well developed at the phenomenological level, and can also be built into codes that predict fracture. The admission of any model for microscopic processes introduces a length scale, and size effects may emerge. These are of practical importance as well as theoretical interest. Mathematical theory based on variational methods is developing, at least for cracks in elastic media. However, many problems remain: there is no adequate theory for the stability of a propagating crack, even in the framework of linear elasticity, at the present time.

It is intended here to develop and improve fracture model (Stiffness Release Model, [19,20]) for simulating high-speed crack.

3.2 Methods for Simulation of Dynamic Crack Propagation by Finite Element Method

To simulate a crack propagation in solids two different concepts of finite element modeling are in use i.e., stationary mesh procedure and moving mesh procedure. Out of these two, moving mesh procedure, as the name implies involve change of mesh in each step as the crack propagates. This is computationally very intensive. Stationary

mesh procedures do not require changes in the mesh in general, and require only change in the boundary and loading conditions. The two procedures are explained in the following sections.

3.2.1 Stationary Mesh Procedure

In the simple stationary mesh procedure of modeling linear elastodynamic crack propagation, the nodes ahead of the crack tip are spaced at $V_c\Delta t$ (V_c being crack velocity) and crack propagation is simulated by releasing the nodes one at a time. However, if a simple node release technique is used, release of constraint on the displacement (at the preceding crack tip) in each time step induces spurious high frequency oscillations in the finite element solution. To overcome these difficulties, several algorithms have been suggested in the literature to release the node gradually over few time steps.

Keegstra et al. [25, 26] suggested a model in which node was not released instantaneously when the force at the crack tip reaches a critical value F_D, which is proportional to dynamic fracture toughness K_D. Instead the force was reduced from F_D gradually in accordance with an elastic spring model so that the nodal force vanishes when critical displacement is reached. Another node release technique of gradual release of nodes is 'Force release model' which is described below.

3.2.1.1 Force Release Model

Suppose that the actual tip is located at 'C' in between the finite element nodes B and D as shown in Figure 3.1. The length segments BC and BD are b and d respectively. The holding back force, F, at node B is gradually reduced to zero over a number of time steps as the crack tip reaches to the node D. Various schemes available to decrease the force to zero are as follows:

(i) Malluck and King [27] suggested the release rate based on constant stress intensity factor

$$\frac{F}{F_0} = \left(1 - \frac{b}{d}\right)^{\frac{1}{2}} \tag{3.1}$$

where F_0 is the original reaction force when the crack tip was located at node B.

(ii) Rydhom et al. [28] Suggested the release rate based on constant energy release rate

$$\frac{F}{F_0} = \left(1 - \frac{b}{d}\right)^{\frac{3}{2}} \tag{3.2}$$

(iii) Kobayasi et al. 29] suggested the linear release rate based on no physical argument other that pure intuition.

$$\frac{F}{F_0} = \left(1 - \frac{b}{d}\right) \tag{3.3}$$

In order to have more gradual and smooth propagation of crack Kishore, Kumar and Verma [30] used a modified method. Holding back force at the crack tip B is linearly decreased to zero when the crack reaches the end of the next element. Thus when crack tip goes beyond node B then

$$\frac{F_B}{F_{HB}} = \left(1 - \frac{b}{d + d_1}\right) \tag{3.4}$$

where F_{HB} is the reaction at node B, when the node was closed, b is the crack extension and d, d_1 are the length of the elements as shown in Figure 3.1. And when the crack moves beyond node D to a point D_1

$$\frac{F_B}{F_{HB}} = \left(1 - \frac{d + b_2}{d + d_1}\right) \tag{3.5}$$

$$\frac{F_D}{F_{HD}} = \left(1 - \frac{b_2}{d_1 + d_2}\right) \tag{3.6}$$

where F_{HD} is the reaction at node D, when the node was closed. b, b_2 are the crack extension and d, d_1, d_2 are the element lengths as shown in Figure 3.1

In force release model, time increment Δt is usually taken such that it takes 15 to 20 iterations for the crack tip to cross one element. The amount of force necessary to keep the nodes together is determined and a factor is used to proportionately decrease the force as the crack tip advances. Thus, at subsequent times, though the problem is highly dynamic, the current calculations were based on the force calculated to keep the nodes together 15 to 20 time steps before. This will cause discrepancy as the crack advances further from one element to the next one causing large oscillations in the solution. This discrepancy should be overcome for obtaining better solution. A new model is proposed to overcome the drawbacks of force release model that instead of considering dynamic force at the crack tip takes into account the stiffness and mass of the element at the crack tip. It is described in detail in the later part of this chapter.

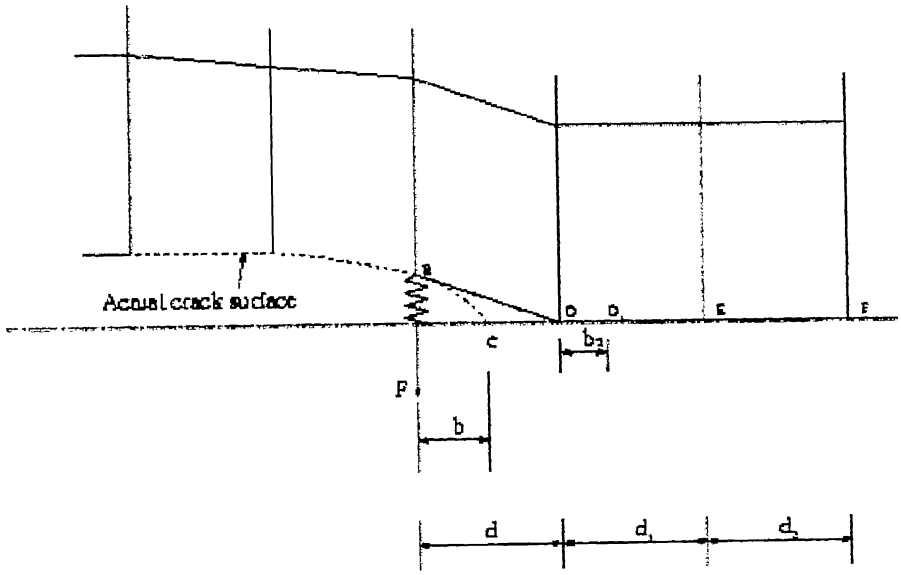

Figure 3.1 Crack opening scheme in force release model

3.2.2 Moving Mesh Procedure

In moving mesh procedure, entire mesh moves with the crack tip. It can be further classified into an approach wherein a) the entire mesh moves b) only the mesh in a finite and small region around the crack-tip moves along with the crack-tip. Aberson et al. [31, 32] used a singular crack-tip element as shown in Figure 3.2(a), which incorporates the first 13 terms of Williams' eigenfunctions [33], appropriate to a stationary crack in a linear elastic body. The crack tip moves within the singular element, between the nodes A and B as shown in Figure 3.2(a). When the crack tip reaches the node B, the mesh pattern is changed suddenly, as illustrated in the figure.

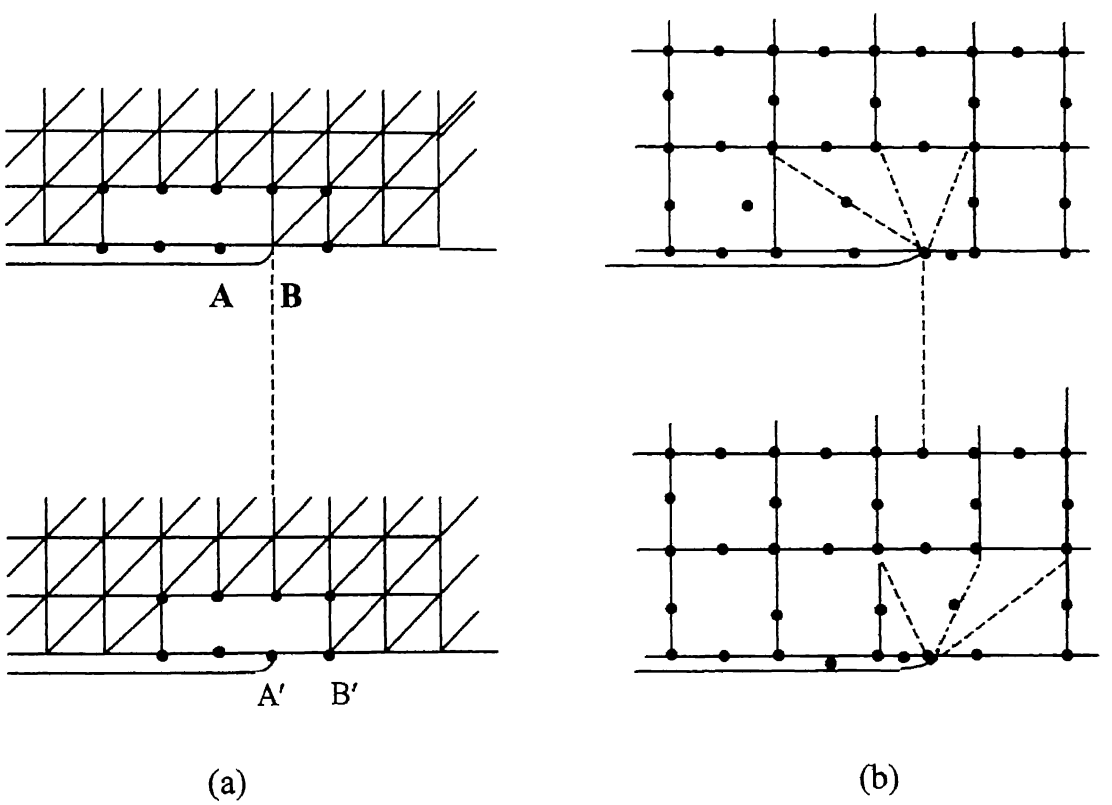

Figure 3.2 Discontinuously moving singular elements

Another attempt at using Williams' eigenfunctions was made by Patterson and Oldale [34, 35]. The singular element (Figure 3.2(b)) has 13 nodes and is topologically equivalent to two assembled 8 noded isoparametric elements. The location of the singular element is suddenly changed by a distance equal to the size of the regular element ahead of the crack tip, when the crack tip propagates a critical distance within the singular element. The displacements of the singular element are matched to those of the surrounding solid only at the nodes connected to the regular element. Thus, this model violates the displacement compatibility condition at the interfaces between the singular element and the surrounding regular elements. In another procedure, the singular element translates in each time step for which crack growth occurs. Thus crack tip is always at the center of the singular element throughout the analysis. The regular elements surrounding the moving singular element are continuously distorted. Mesh pattern around the singular element is periodically readjusted for simulating large amount of crack propagation.

3.3 Stiffness Release Model for Crack Propagation

The force release models to simulate crack propagation as applied to high-speed crack propagation has the following drawbacks:

1. They give rise to very high oscillations in the solution.
2. They are not suitable for solving inverse problem in crack propagation. If the crack propagates and stops in between an element and starts again later when another stress wave arrives, how much holding force to be used is not known.

The time increment Δt, is usually taken such that it takes 15 to 20 iterations for the crack-tip to cross one element. The amount of force necessary to keep the nodes together is determined and a factor is used to proportionaly decrease this force as the crack advances. Thus, at subsequent times, though the problem is highly dynamic, the current calculations were based on the force calculated to keep the

nodes closed 15 to 20 time steps before. This will cause discrepancy as the crack advances further results in large oscillations in the solution.

In the case of decreasing energy release rate and possible crack arrest in between the nodes, using the force at particular value in the propagation problem will lead to a non-acceptable solution. This aspect acquires importance in the case of inverse problems.

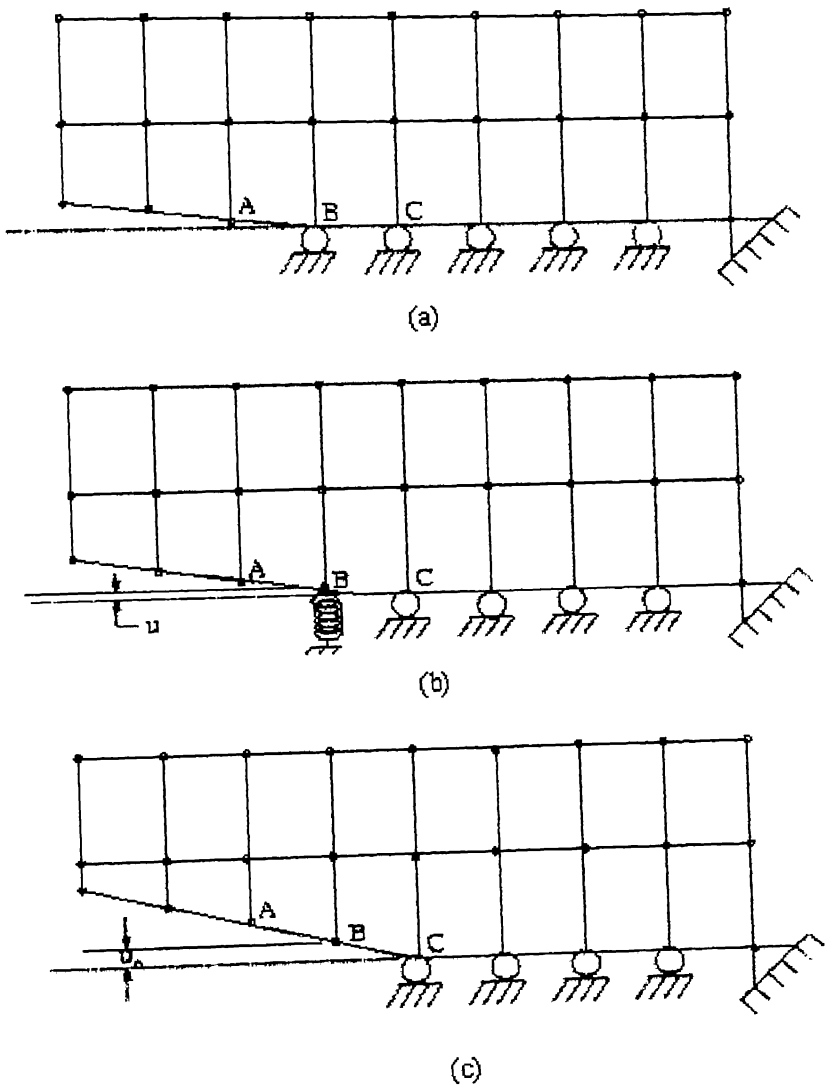

Figure 3.3 Crack opening scheme in stiffness release model

In the present work, a propagation model with modified stiffness and mass matrices is presented to take into account the extension of crack in plates. In stiffness release model [19, 20], one-dimensional elastic element is added at the crack tip node, whose stiffness is reduced gradually as crack tip advances to the next node (Fig 3.3). Additional stiffness required is very large when crack tip is at the beginning of element and zero when crack tip reaches to the other end. Amount of additional stiffness required is a function of crack length and is obtained from quasi-static crack propagation analysis.

Figure 3.3(a) shows a symmetric part of a deformed plate in which crack is up to the node B. Figure 3.3(c) shows the configuration of the plate when the crack has completely propagated to the next node C. Figure 3.3(b) shows the modelling of the plate with partially propagated crack (some where between B and C) by the addition of a one-dimensional linear spring element whose stiffness is K_s.

Let,

K_0 be the stiffness at node B of original plate without additional spring

u_0 be the displacement of node when crack tip reaches the next node and element opens up completely.

K_s can be found out from equilibrium equation as

$$\mathbf{K}_0(\mathbf{u}_0 - \mathbf{u}) = \mathbf{K}_s\mathbf{u} \tag{3.7}$$

$$\boldsymbol{K}_s = \boldsymbol{K}_0\left[\frac{\boldsymbol{u}_0}{\boldsymbol{u}} - 1\right] \tag{3.8}$$

Energy in the spring is given as

$$E_s = \frac{1}{2}K_s u^2 = \frac{1}{2}K_0\left[\frac{u_0}{u} - 1\right]u^2 \tag{3.9}$$

Energy release rate is written as

$$\boldsymbol{G} = \frac{\Delta \boldsymbol{E}}{\Delta \boldsymbol{A}} \tag{3.10}$$

where ΔA is the increment in crack area

Let a non-dimensional parameter for crack length (a) be defined as,

a=crack length (within element) / d

where d is the distance between two nodes.

$\therefore \Delta A = Bd\Delta a$

where B is the thickness of plate.

For static case, energy release rate can be written as

$$G = \frac{1}{2} K_0 (-u_0) \frac{1}{Bd} \frac{du}{da} \tag{3.11}$$

Assuming linear variation of G and a, G can be written as

$$G = C_1 + C_2 a \tag{3.12}$$

where, C_1 and C_2 are the constants to be determined.

Substituting G in Equation (3.11)

$$C_1 + C_2 a = -\frac{1}{2} \frac{K_0 u_0}{Bd} \left(\frac{du}{da} \right) \tag{3.13}$$

On integrating Equation (3.13), we get

$$u = -\frac{2}{K_0 u_0} Bd \left(C_1 a + \frac{C_2 a^2}{2} + C_0 \right) \tag{3.14}$$

On substituting initial condition u=0 when a=0 and

end condition $u=u_0$ when a=1

$$u_0 = -\frac{2}{k_0 u_0} Bd \left(C_1 + \frac{C_2}{2} \right) \tag{3.15}$$

Equation (3.14) and Equation (3.15) gives

$$\frac{u}{u_0} = \frac{2C_1 a + C_2 a^2}{2C_1 + C_2} \tag{3.16}$$

On simplification it reduces to

$$\frac{u}{u_0} = a + C(a - a^2) = f \tag{3.17}$$

where

$$C = -\left(\frac{C_2}{2C_1 + C_2}\right) \tag{3.18}$$

Equation (3.8) finally can be written as

$$K_s = K_0\left(\frac{1-f}{f}\right) \tag{3.19}$$

where $f=u/u_0$ as given by Equation (3.17)

Static stiffness K_0 can be determined for a given specimen under static condition. Energy release rate is determined using Equation (3.11) and (3.17).

However as Equation 3.11 was based on quasi-static crack propagation, it doesn't take into account the kinetic energy in the body. In dynamic problem total energy comprise strain energy in the body, kinetic energy and work done by external forces. For finding energy release rate, drop in the total energy in the system is considered in the present model and energy release rate is determined using fundamental Equation 2.19.

3.4 Effect of Constant 'C'

As can be seen, K_0 has to be determined for the given plate under quasi-static conditions and given boundary conditions. However, it may be inferred that the near boundaries affect the value of K_0 more than the far off boundaries. Suitable value of

'C' can be determined by trial and error to obtain continuous energy release rate in between elements. For a quasi-static case usually it is a very small value. In the present problem, it is of the order of 0.25.

However, it was observed that C has considerable effect on the dynamic crack propagation. Effect of change in value of C on f vs. non-dimensional crack length, a is shown in Figure (3.4)

Spring stiffness, K_s that is gradually reduced as the crack propagates, is a function of crack length 'a' and constant C as shown in Figure (3.5). Figure (3.5) shows that C plays major role in controlling the value of K_s. Also constant, C is affected by change in element size and time step Δt. For a given problem, its value needs to be chosen so that final energy release rate curve are smooth without wide fluctuation. Although the proposed stiffness K_s of the additional elastic spring element varies from $\propto$ to 0, it changes discretely in a finite number of steps as the crack propagates through one element.

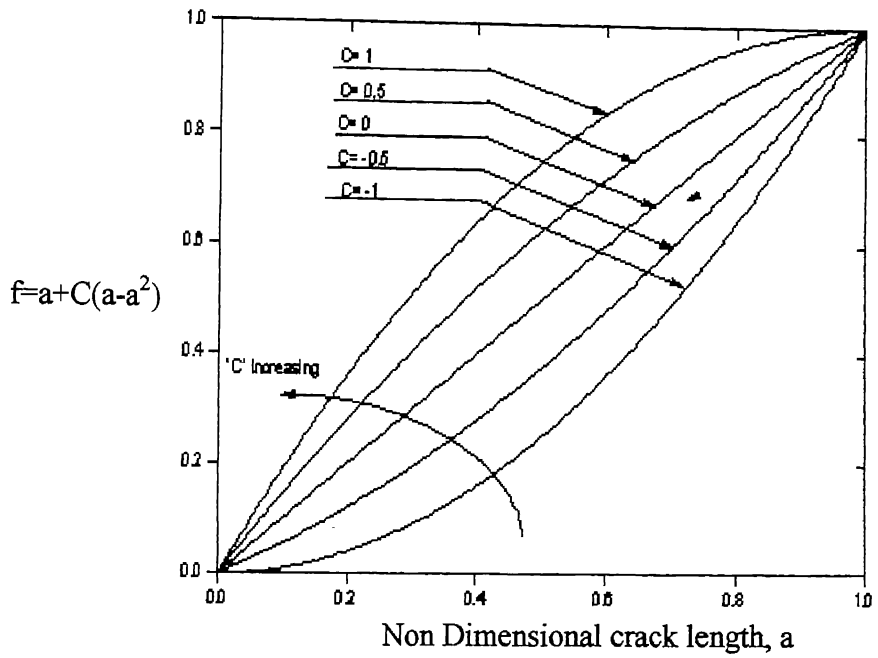

Figure 3.4 f vs. a curve for different C

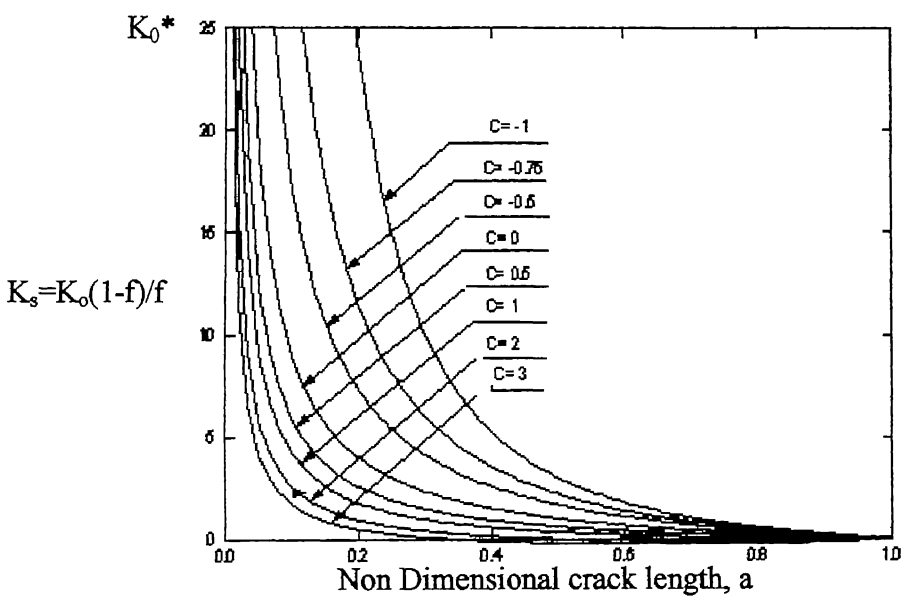

Figure 3.5 K_s vs. a, for different C

3.5 Improved Stiffness Release Model

Figure 3.5 shows that the variation in the stiffness, K_s depends on the value of 'C', which also affects the energy release rate, G. The fluctuation in the energy release rate at element boundaries changes with the values of 'C'. In order to have less fluctuation at the element boundaries one has to play with different values of 'C' and by trial and error method 'C' is chosen which has least fluctuation.To overcome this difficulty, improved stiffness release model is proposed as:

$$f' = a + C(a - a^2)^{\alpha} \tag{3.20}$$

where α is an exponent.

$$K_s = K_0\left(\frac{1-f'}{f'}\right) \tag{3.21}$$

For α=1, Equation 3.20 represents original stiffness release model [19, 20]. Primary requirements for spring stiffness are as follows:

$K_s \to \infty$ as $a \to 0$ and K_s=0 at $a = 1$. The effect of the parameter α on the stiffness release model as well as on the energy release rate will be discussed in the next chapter.

3.6 Mass Modification

In the stiffness release model [19, 20], as crack propagates, stiffness of the element decreases but mass matrix of the element remains constant. In reality when the crack is at the beginning of the element, there is no mass to get accelerated and the effective mass increases gradually as the crack reaches to the end of the element. At the end of the element, it becomes equal to the mass of the element. To account for this shape functions of the elemental mass matrix at the crack tip are modified so that nodal masses vary as a function of non-dimensional crack length, a.

3.6.1 Modification of Shape Function and the Crack Tip Mass Matrix

Consider the element at the crack tip as shown in Figure 3.6 with the crack partially propagated by an amount 'a' within the element.

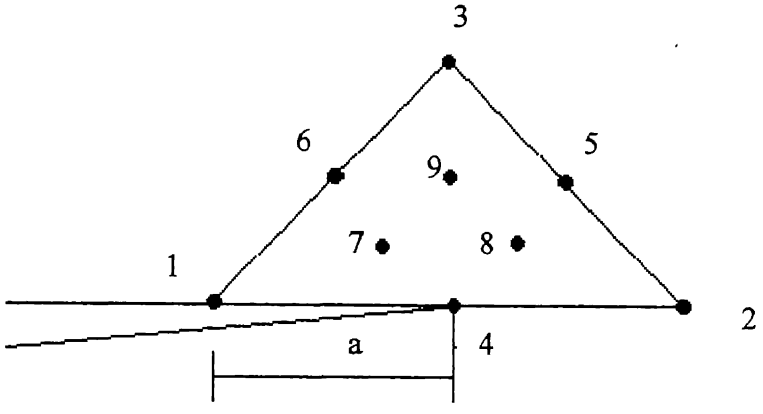

Figure 3.6 Representation of an element at the crack tip

For a 9-noded triangular element the shape functions are given as:

$$
\begin{aligned}
N_1 &= 2L_1^2 - L_1 & N_6 &= 4L_3L_1 \\
N_2 &= 2L_2^2 - L_2 & N_7 &= -32L_1^2 L_2L_3 \\
N_3 &= 2L_3^2 - L_3 & N_8 &= -32L_1L_2^2L_3 \\
N_4 &= 4L_1L_2 & N_9 &= -32L_1L_2L_3^2 \\
N_5 &= 4L_2L_3
\end{aligned}
\qquad (3.22)
$$

The variation of the shape function, N_1 is shown in Figure 3.7

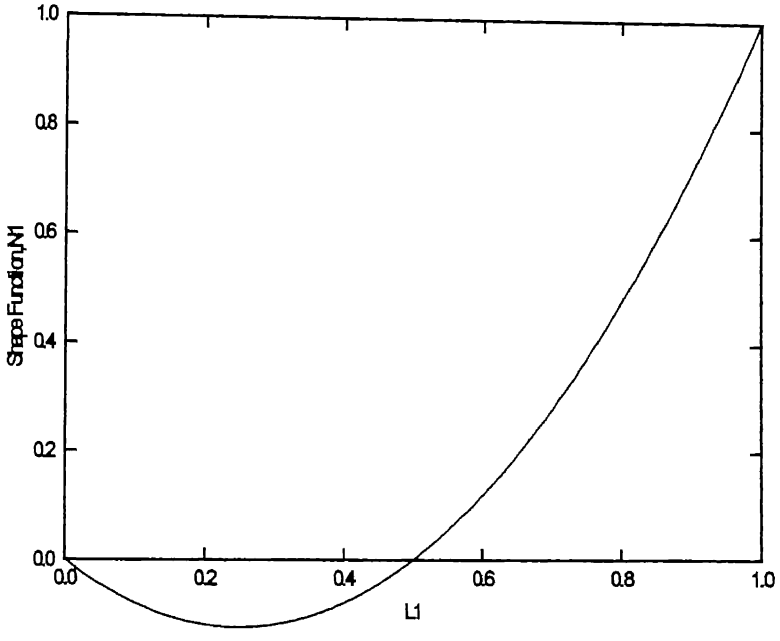

Figure 3.7 Shape Function, N_1 vs. L_1

The shape function, N_1 of the crack tip node is proposed to be a function as,

$$N_1 = (2L_1^2 - L_1)^{\beta} \tag{3.23}$$

where,

$$\beta = \left[\frac{10(1.1-a)}{a}\right]^r \tag{3.24}$$

, a is non-dimensional crack length and r is an index.The function β is chosen such that $\beta = 1$ at a=1 and very high [$\beta \to \infty$ as $a \to 0$] at beginning of the element as shown in Fig 3.8.

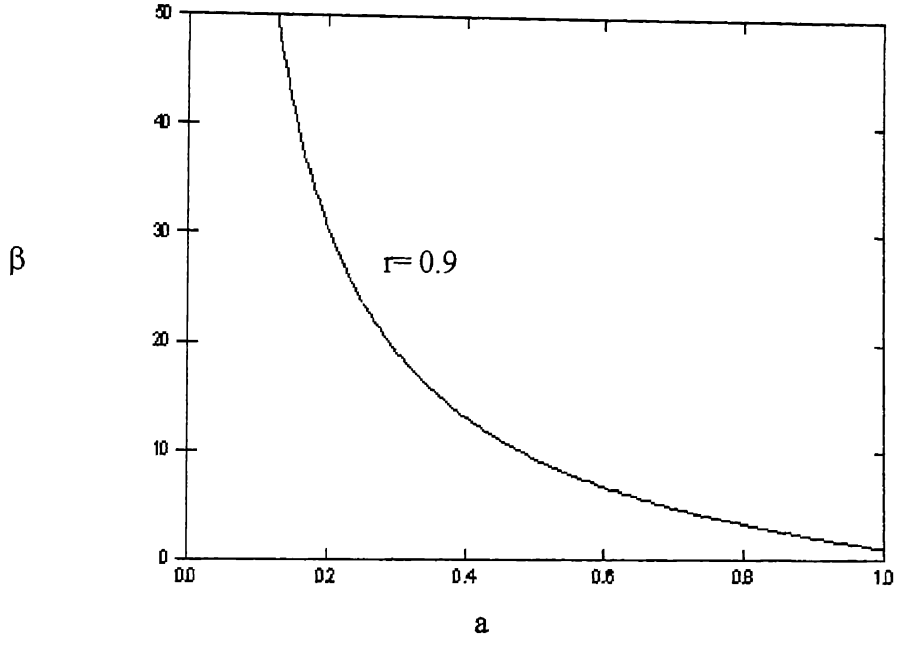

Figure 3.8 β vs. Non-dimensional Crack Length, a

Thus, as the crack advances, the nature of the shape function, N_1 varies in such a way that mass of the element increases gradually. Fig 3.9 shows variation of N_1 at different values of 'a' which shows that area under N_1 increases from zero (at a=0) to maximum final value 1/6 (at a=1). The proposed shape function N_1 along with β is justified at the end of this chapter.

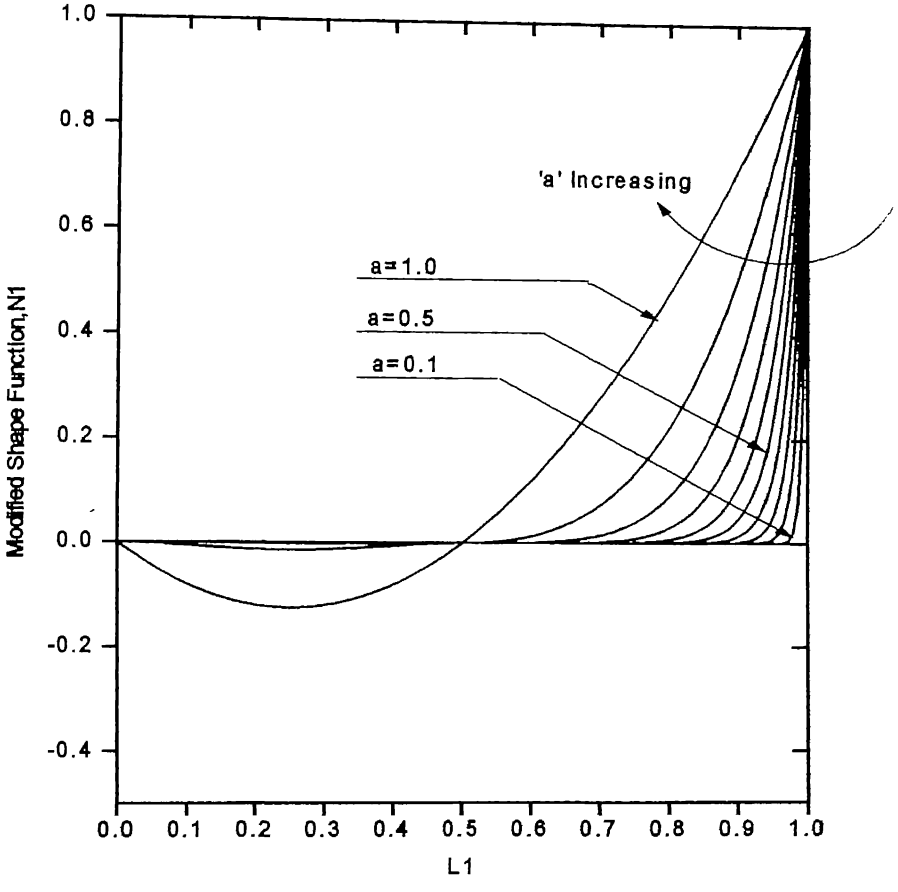

Figure 3.9 Modified Shape, N_1 vs. L_1 for different values of 'a'

3.6.1.1 Modified Mass Matrix, [M]:

$$[N_\theta]=\begin{bmatrix} N_1^\beta & 0 & N_2 & 0 & N_3 & 0 & N_4 \ldots\ldots & N_9 & 0 \\ 0 & N_1^\beta & 0 & N_2 & 0 & N_3 & 0 \ldots\ldots & 0 & N_9 \end{bmatrix}_{(2\times 18)} \quad (3.25)$$

$$[\mathrm{Rmi}]_{(18\times18)} = [\mathrm{N}_\theta]^{\mathrm{T}}[\mathrm{N}_\theta] \tag{3.26}$$

Similarly,

$$[N_w] = \begin{bmatrix} N_1^\beta & N_2 & N_3 & N_4 & N_5 & N_6 \end{bmatrix}_{(1\times6)} \tag{3.27}$$

$$[Rmm]_{(6\times6)} = [N_w]^T[N_w] \tag{3.28}$$

where, N_θ and N_w are shape functions for the nodal variables $\bar{\theta}$ and $\overline{w}$ respectively.

$$[E]_{(18\times18)} = \frac{\rho h^3}{12}\int_{\Omega^{(e)}} N_\theta^T N_\theta d\Omega \tag{3.29}$$

$$[F]_{(6\times6)} = \rho h \int_{\Omega^{(e)}} N_w{}^T N_w d\Omega \tag{3.30}$$

where,

ρ is density of the material,

h is thickness of the plate.

Finally modified mass matrix is given as [Section 2.2],

$$[\mathrm{RM}]^{(e)} = \begin{bmatrix} [\mathrm{E}]_{(18\times18)} & 0 \\ 0 & [\mathrm{F}]_{(6\times6)} \end{bmatrix}_{(24\times24)} \tag{3.31}$$

Equation 3.24 shows that β depends on the index r. Figure 3.10 shows how β varies with index r and Figure 3.11 shows the variation of RM (1,1) as function of non-dimensional crack length, a, within the element. From Figure 3.11 it can be seen that for r=0.9, the variation in element mass matrix is smooth.

By modifying shape function of elemental mass matrix, mass of the element is made to vary as a function of crack length such that the element mass is zero when the crack is at the beginning of the element and increases gradually till crack reaches to the end of the element, when mass of the element becomes equal to the mass of a regular element. Effect of this modification on energy release rate variation will be shown in chapter 4.

3.7 Prediction of Crack Initiation, Propagation and Arrest

The present method can be applied to predict the crack propagation history under the known applied loads, if crack propagation resistance of the material is known. That means that fracture resistance of the material, G as a function of crack propagation velocity is supposed to be a known input data. At each time step, the available energy release rate is determined and it is compared with the material fracture resistance data to predict the crack propagation velocity. This is used to determine the crack propagation length in the given time interval and propagated accordingly. This procedure continues till crack arrest takes place.

3.8 Closure

In this chapter various methods of simulating dynamic crack propagation with stationary and moving mesh are described. The variation of various aspects of the proposed model is also discussed in detail. This model will be investigated with hypothetical data in chap 4. The effect of various parameters on energy release rate will be described in the succeeding chapter.

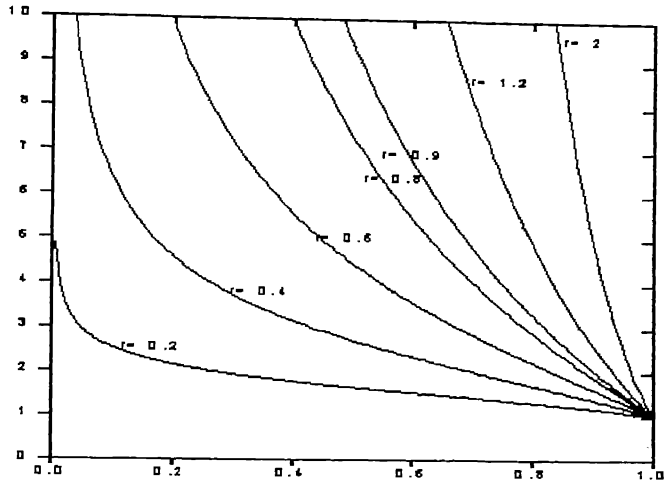

Figure 3.10 β vs. Non-dimensional crack length, a for different values of r

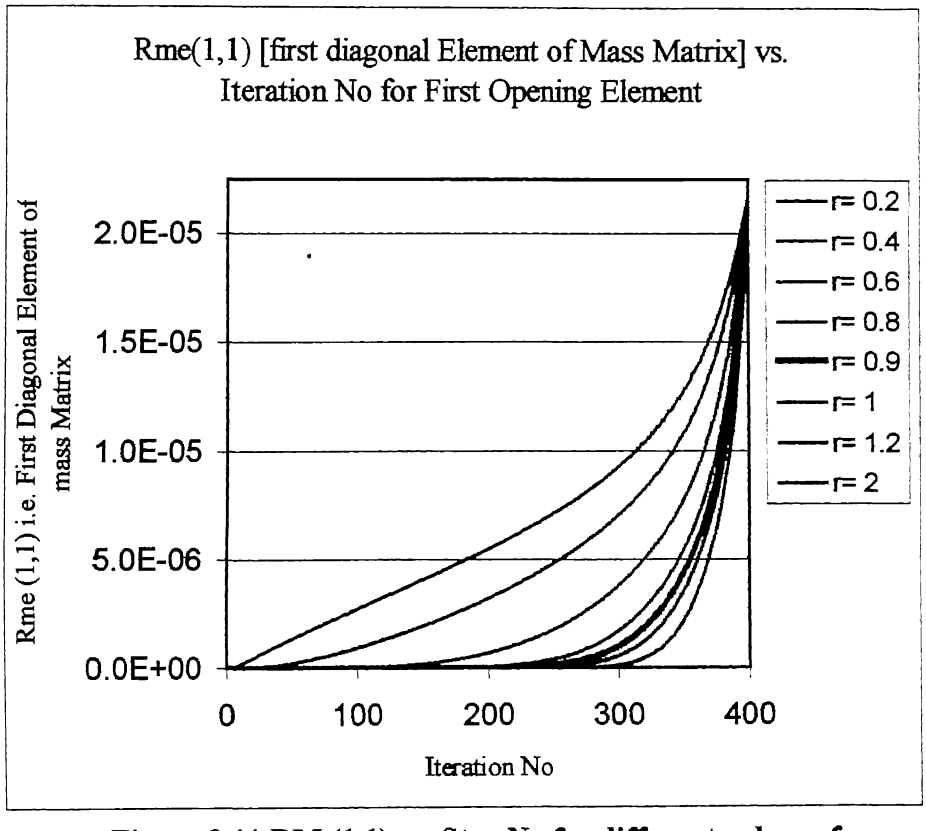

Figure 3.11 RM (1,1) vs. Step No for different values of r

CHAPTER 4

RESULTS AND DISCUSSION

4.1 Introduction

This chapter is concerned with the validation of the method and demonstrate the effect of improved stiffness release model along with mass modification on energy release rate and other fracture parameters. First FEM code developed is validated for static case. Later problems with a typical data are considered to discuss the effect of crack propagation model parameters along with mass modification on energy release rate, G. Finally a plate with a crack is analysed as:

1. Forward problem and
2. Inverse problem

in which plate subjected to impact loading is analysed by using the 9-noded hybrid triangular elements.

4.2 Validation for Static case

A plate without crack with all the four edges simply supported subjected to a uniformly distributed loading is analysed by the FEM code with the 9-noded hybrid triangular element and the results are compared with theoretical values.

Dimensions of the plate: Length, L= 3 m and width, W= 2 m.

The final refined mesh used is shown in Figure 4.1.

The maximum deflection of the plate at its centre is given by the formula (Timoshenko, 1959, [24])

$$w_{max} = (\alpha\, q\, a^4)/D$$

where, $D = E^*h^3/12(1-\vartheta^2)$

E= Young's Modulus of Elasticity

h = thickness of the plate

ϑ = Poisson's ratio

α = Numerical factor depending on the ratio b/a of the sides of the plate (for a uniformly loaded plate with the 4-edges simply supported)

= 0.00772

q = uniformly distributed load

a = length of plate in x-direction= 2 m

b = length of plate in y-direction= 3 m

For a steel plate, with E = 200 GPa, h = 0.03 m, ϑ = 0.3, q = 1000 N/m^2, a= 2 m , the above formula gives w_{max} = 2.49 $\times 10^{-4}$ m. The displacement contour obtained by FEM code is shown Figure 4.2.The value of maximum deflection w_{max}, obtained from the code is 2.6×10^{-4} m. It can be observed that the error is 4.4 % for the 54-element mesh.

4.3 Input Parameters for Hypothetical Problems

In this section, the effects of various parameters in the crack propagation model are investigated for the plate subjected to typical load. The material properties, plate geometry, loading, and boundary conditions used for analysis are as follows.

Material properties:

- Modulus of Elasticity, E = 210 GPa
- Poisson's Ratio, v= 0.3
- Density of the material, ρ = 7800 kg/m^3

The rectangular plate is shown in Figure 4.3 has a central crack parallel to Y-axis.

Dimension of the plate:

- Length of the plate, L= 4 m
- Width of the plate, W= 2 m
- Crack Length, (2a)= 0.4 m
- Thickness of the plate, h= 0.024 m

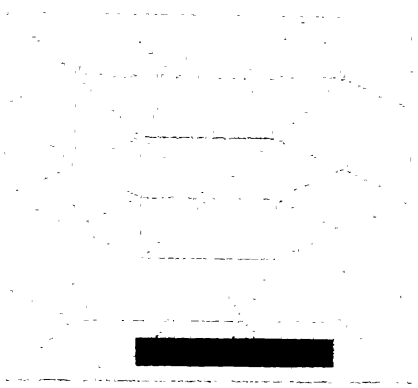

Figure 4.1 Meshing used for static case

Figure 4.2 Displacement Contours for static case

Input Pulse:

The plate is subjected to a uniformly distributed impulse load of intensity, q, which rises sharply and dies down slowly as shown in Figure 4.4 is given by,

$$q = \frac{ampq}{0.3679}\frac{t}{t_{at\_max}}e^{(-\frac{t}{t_{at\_max}})}$$

$$t_{at\_max} = \frac{pdur}{4}$$

where t_{at_max} = Rise time,

pdur = Total pulse time

Details of the input pulse are as follows:

- Amplitude of the Load = 1000 N
- Rise Time = 35 μs

The plate has all the four sides simply supported is analysed as shown in Figure 4.5. As the problem is symmetric about X and Y-axis, only a quarter of the plate as shown in Figure 4.6, is analysed.

Details of meshing as shown in Figure 4.7 is as follows:

- No. of elements= 143
- No. of nodes= 739
- No. of degree of freedom= 1788

Crack Propagation Details:

- No. of element to open = 3
- Time step (dt) = 2 μs
- Load steps: Load steps are the number of steps to open one particular element.

  Load steps for first opening element = 400

  Load steps for second opening element = 240

  Load steps for third opening element = 220

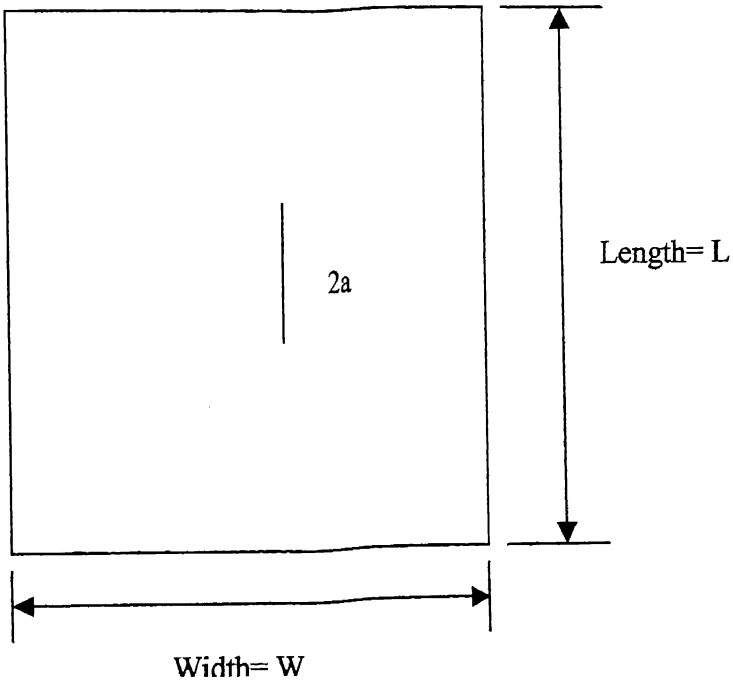

Figure 4.3 Plate Geometry

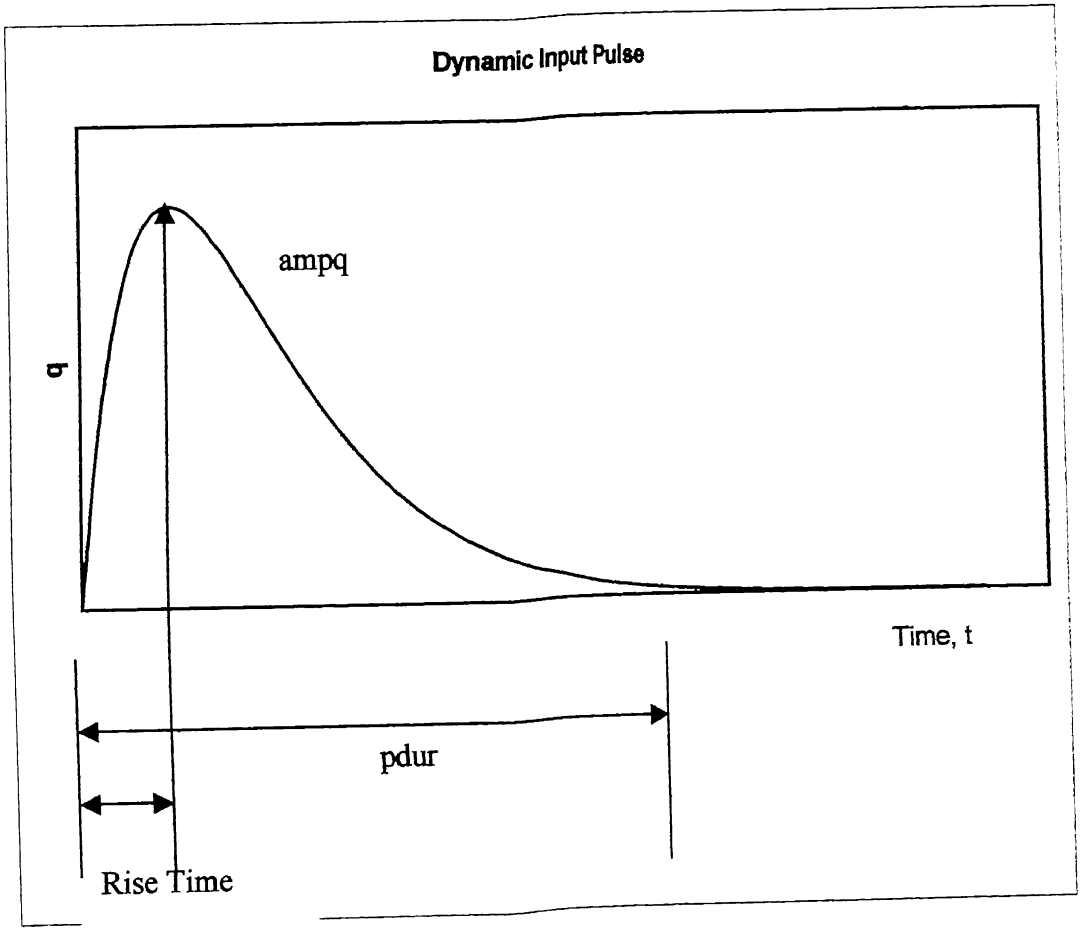

Figure 4.4. Dynamic Input Pulse.

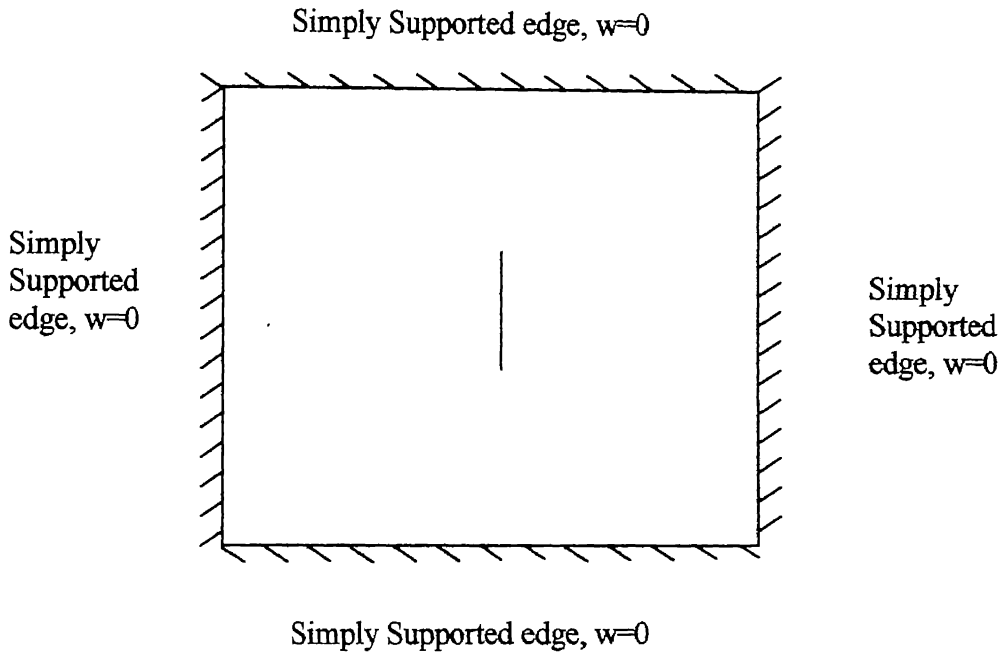

Figure 4.5 Boundary Conditions

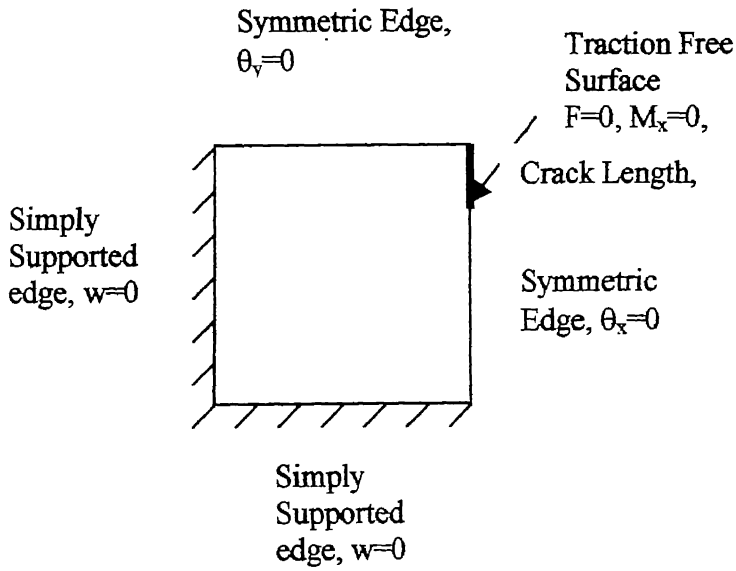

Figure 4. 6 Boundary Conditions for Symmetric Quarter plate

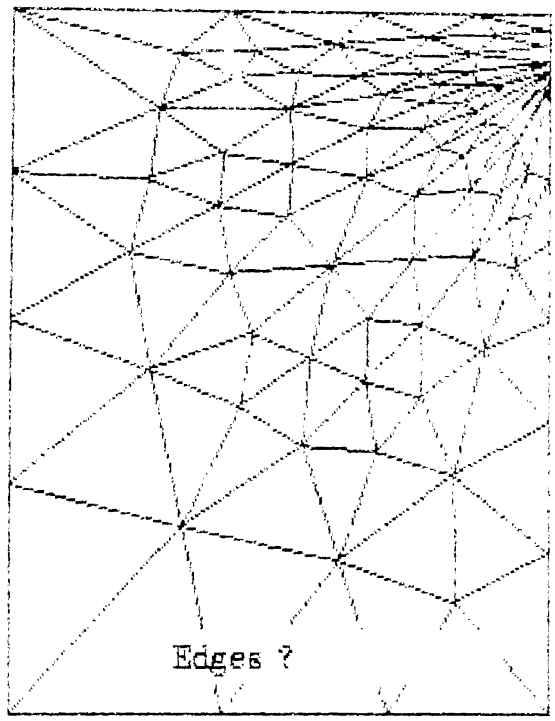

Figure 4.7 Mesh used for Hypothetical Problem

4.4 Results for Improved Stiffness Release Model

4.4.1 Effect of the Parameter α on Spring Stiffness, K_s

In the stiffness release model developed by Kishore, Reddy and Deshmukh [19, 20], the spring stiffness, K_s depends highly on the values of constant 'C' as seen from Figure 3.5. Figure 4.8 shows the variation in energy release rate for different values of 'C'. 'C' plays major role in fluctuations of G at element boundaries. Figure 4.9 and Figure 4.10 show fluctuations at the elemental boundaries. To overcome this difficulty, improved stiffness release model is proposed [Section 3.5] as

$$f' = a + C(a - a^2)^{\alpha} \quad \text{and}$$

$$K_s = K_0\left(\frac{1-f'}{f'}\right)$$

Figure 4.11 to Figure 4.16 shows the variation of K_s vs. non-dimensional crack length, a, for different values of α. For α=1 nature of K_s largely depends on values of 'C'. It is evident from Figure 4.11 that K_s becomes discontinuous at a= 0.5 for C= -2 as f approaches zero. Also for very high values of 'C' (C≥ 2), the stiffness of the spring is completely released when the crack is at the beginning of the element itself, which is not realistic with the nature as stiffness, K_s should release over the whole element. For example at a= 0.5 for C= 2, K_s becomes zero (Figure 4.11).

It is clearly observed that by increasing the value of α, the dependence of spring stiffness, K_s on 'C' value reduces. From Figure 4.13, it can be seen that for α= 2, the range of 'C' value has been increased as compared to α=1 (Figure 4.11) for which the propagation model works satisfactorily. Thus as the value of α increases, the range of 'C' for which model works satisfactorily increases. Hence with increase in α, dependence of K_s on 'C' reduces.

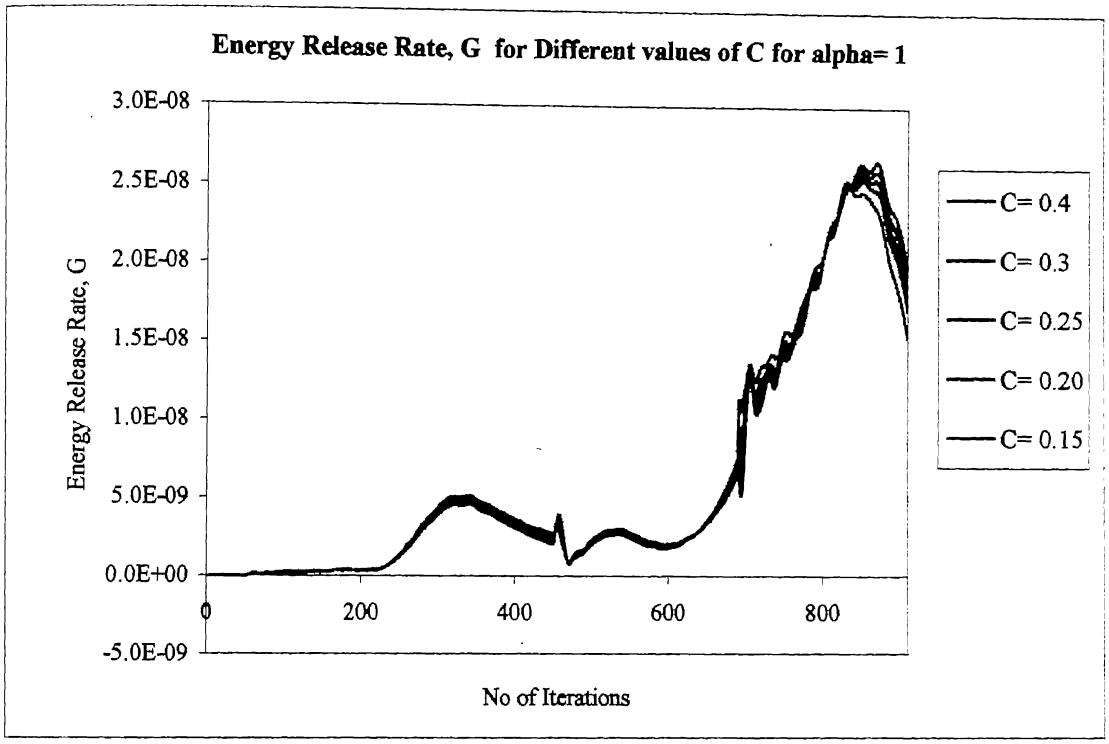

Figure 4.8 Energy Release Rate, G vs. No. of Iterations

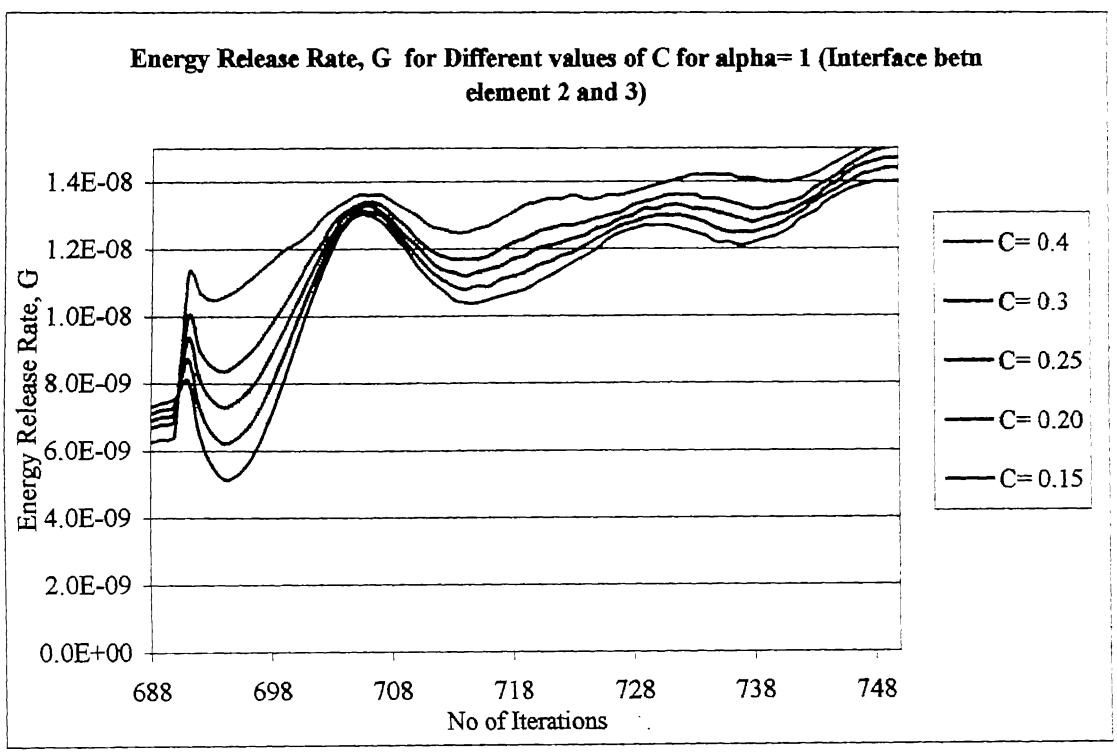

Figure 4.9 Energy Release Rate, G vs. No. of Iterations

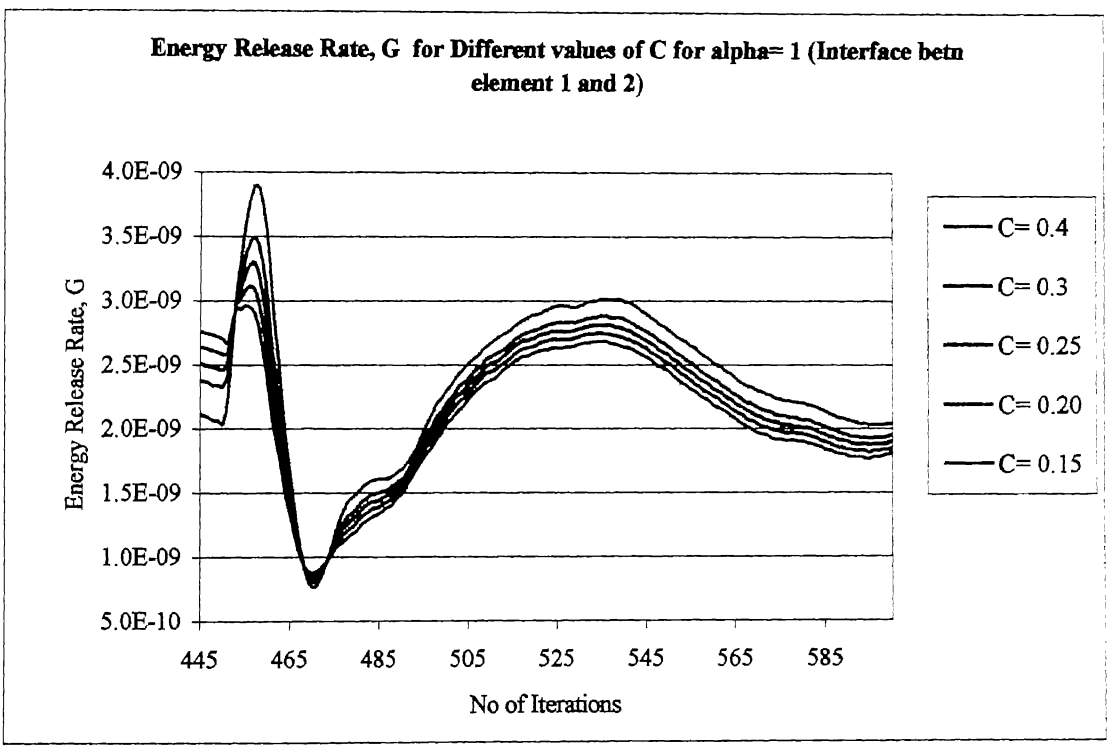

Figure 4.10 Energy Release Rate, G vs. No. of Iterations

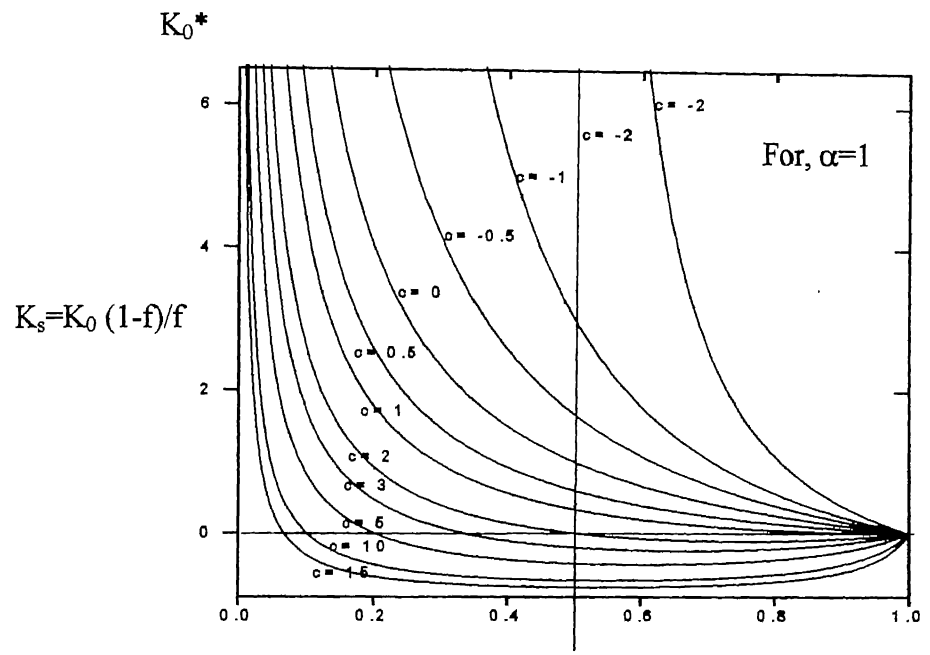

Figure 4.11 K_s vs. a, for different C and α=1

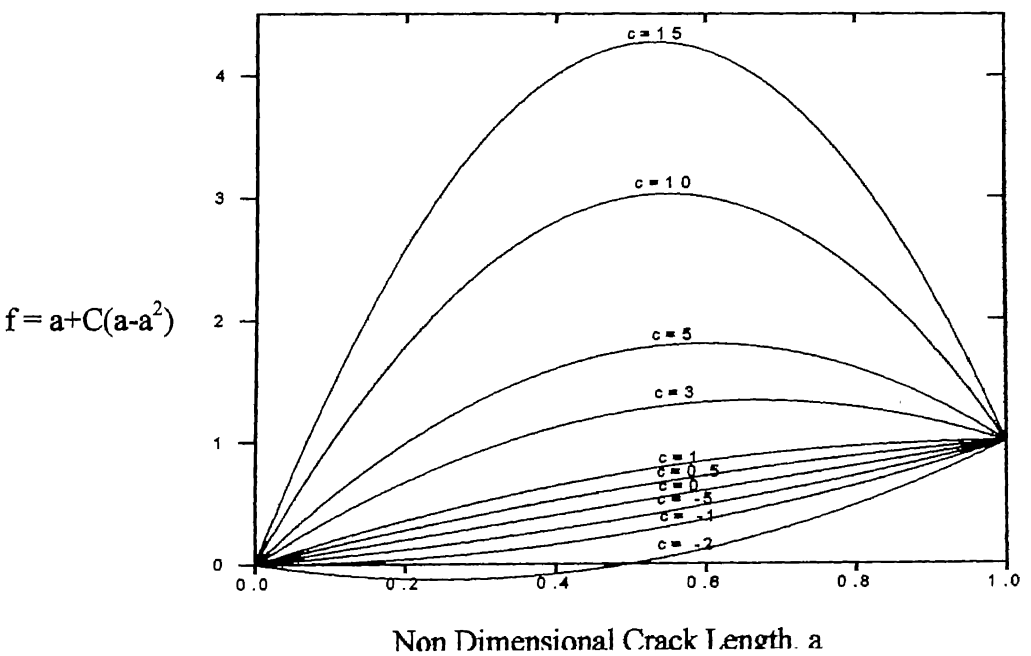

Figure 4.12 f vs. a, for different C and α=1

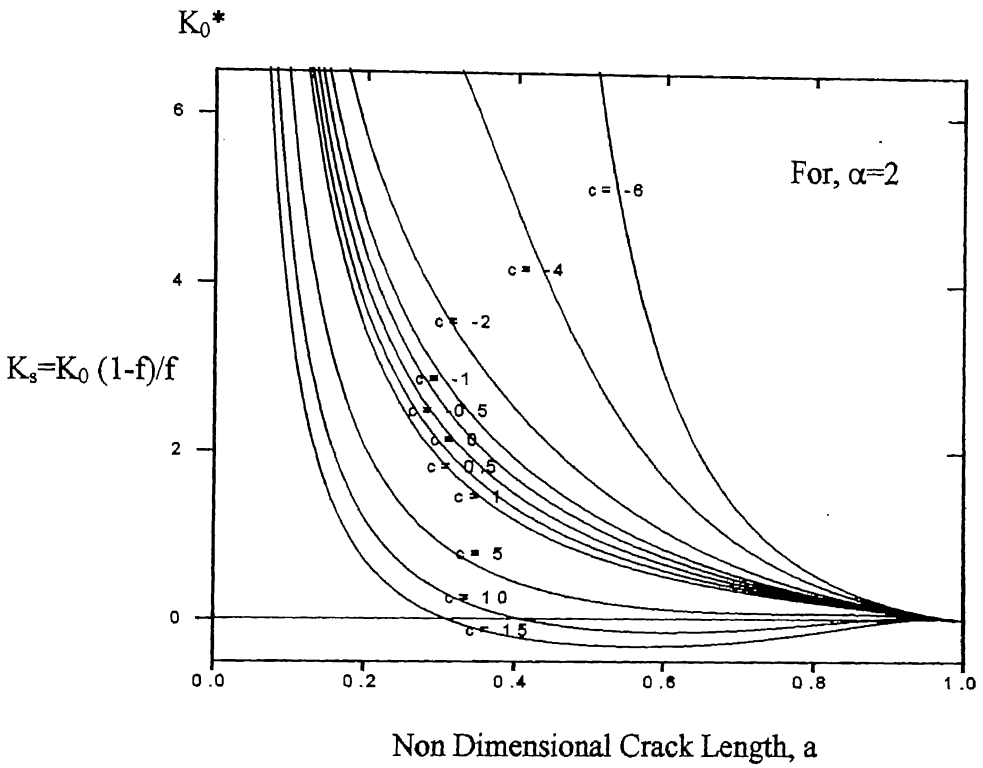

Figure 4.13 K_s vs. a, for different C and α=2

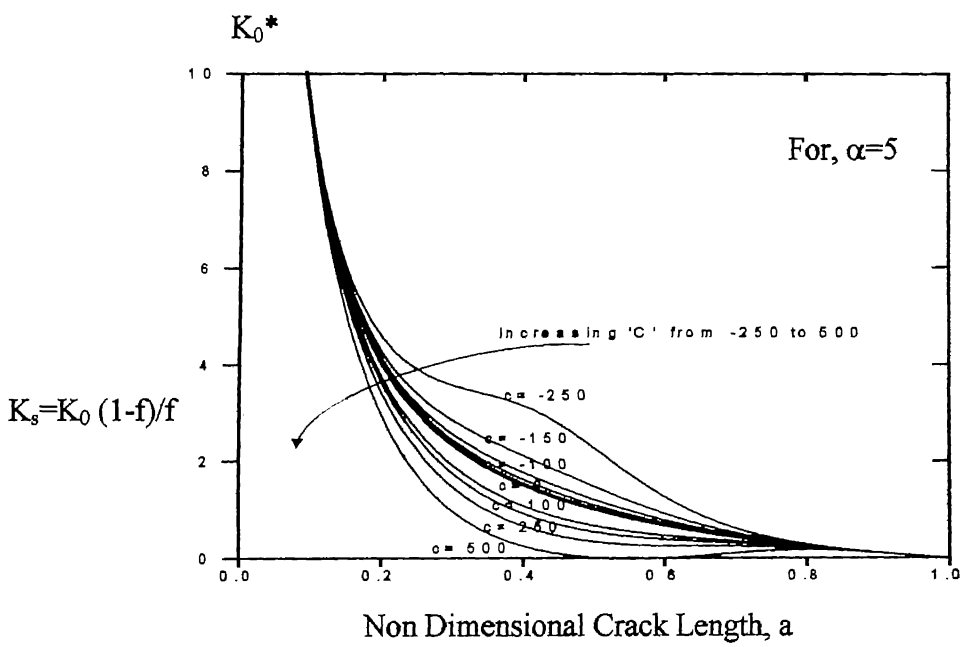

Figure 4.14 K_s vs. a, for different C and α=5

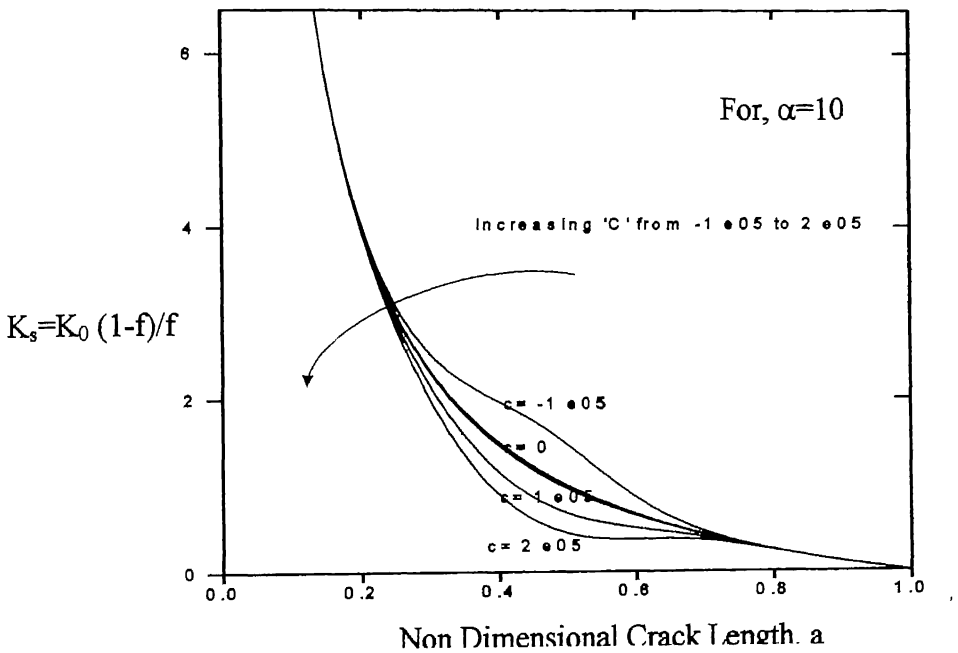

Figure 4.15 K_s vs. a, for different C and α=10

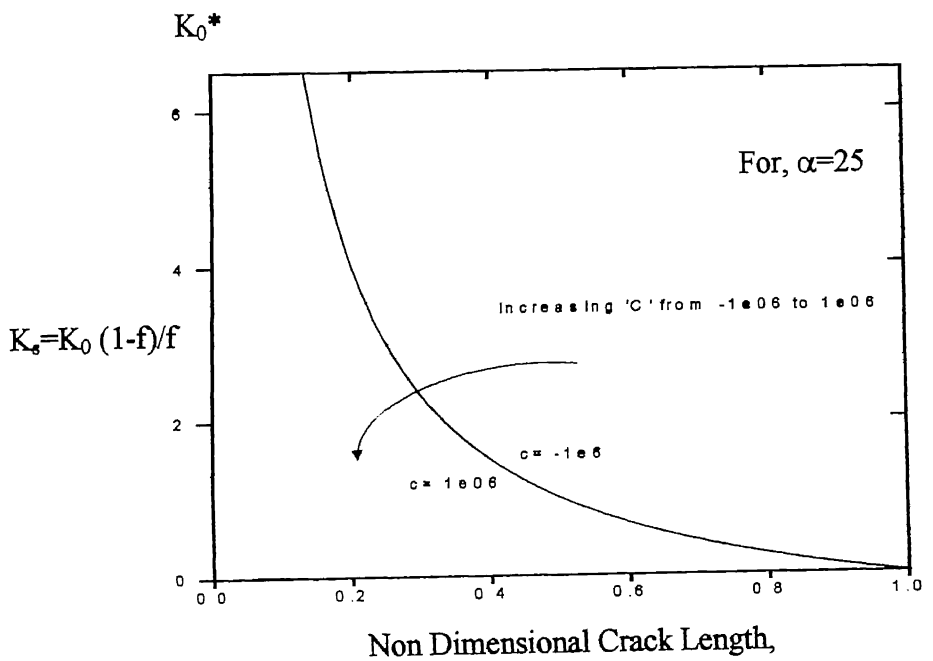

Figure 4.16 K_s vs. a, for different C and α=25

4.4.2 Effect of the parameter α on Energy Release Rate, G

The effect of increase in α on energy release rate is shown in figure 4.17. It is observed that with increase in α, fluctuations in the energy release rate at the element boundaries decreases. The decrease in the fluctuations is faster initially for low values of α and becomes slower for higher values of α as seen from the Figure 4.18. Thus moderate values of α between 2 to 10 are proposed for improved stiffness release model.

4.5 Results for Mass Modification

In stiffness release model [19, 20], 'C' value was chosen such that fluctuations in the energy release rate was minimum. In improved stiffness release model, the dependence of energy release rate on 'C' value as well as fluctuations at the elemental boundaries are reduced by introducing parameter α. Further by mass modification, the fluctuations at elemental boundaries can be still reduced.

As the stiffness of elastic element decreases gradually to zero, the element mass can be increased from zero to its usual value by modifying shape function N_1 for an element containing propagating crack (Section 3.6.1). Energy release rate after this mass modification is shown in Figure 4.19. Figure reveals that final energy release rate curve gives smooth variation within element and fairly stable solutions across element boundaries.

Figure 4.20 shows energy release rate with and without mass modification. It can be seen very clearly that solution with mass modification is better than one without mass modification (Figure 4.21 and Figure 4.22). Thus mass modification gives smooth variation in energy release rate within element as well as at the element boundaries.

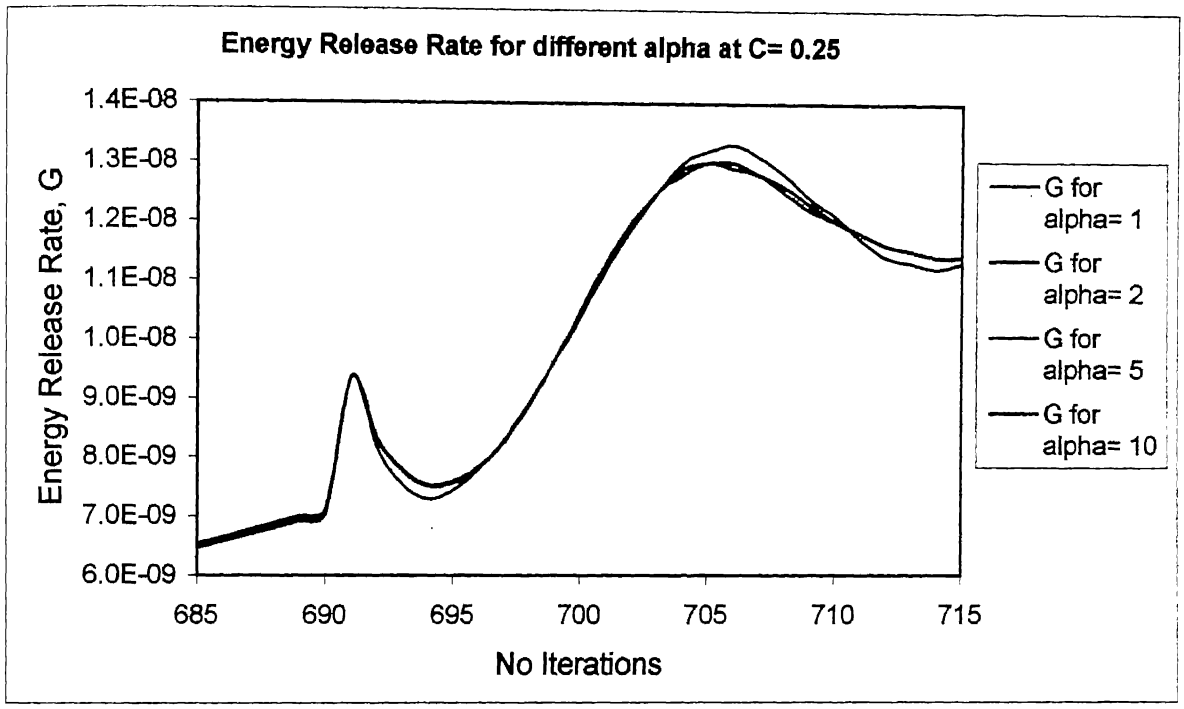

Figure 4.17 Energy Release Rate, G vs. No. of Iterations

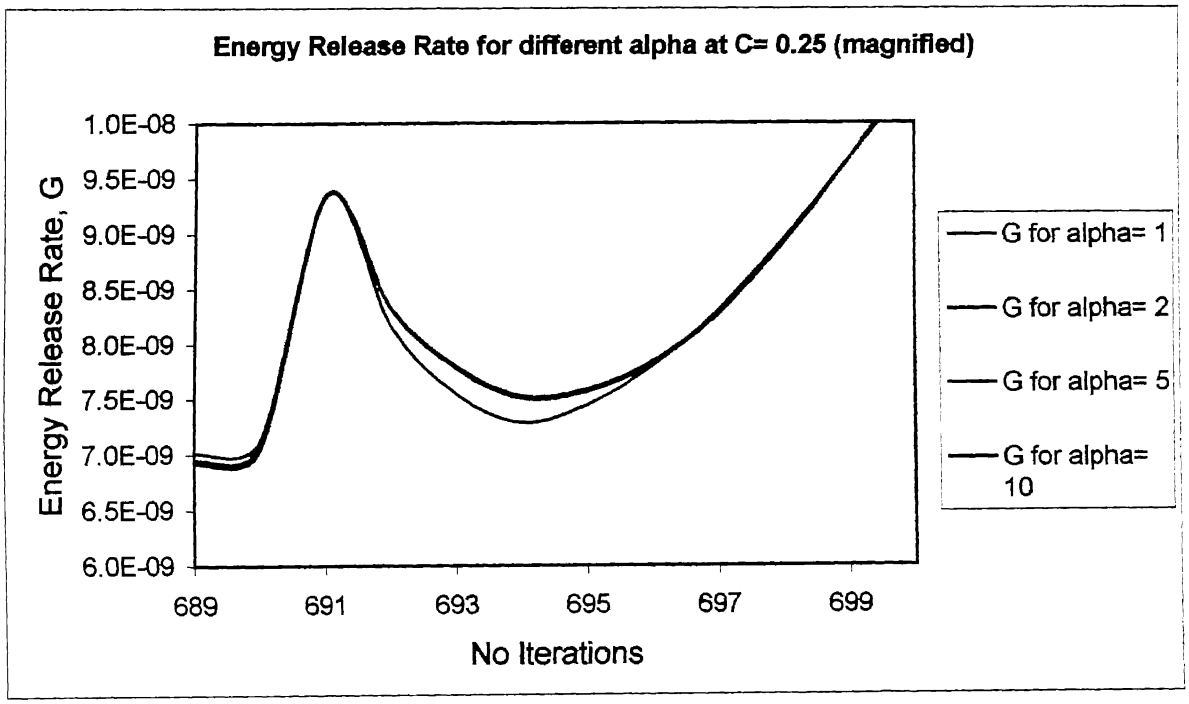

Figure 4.18 Energy Release Rate, G vs. No. of Iterations

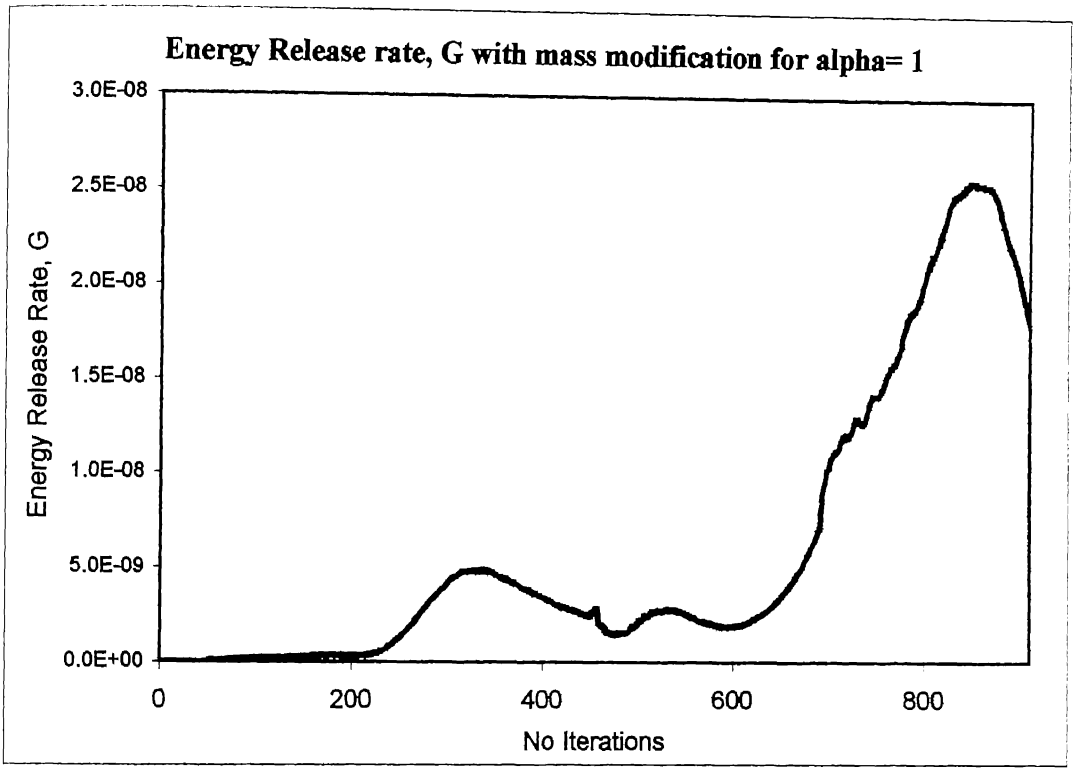

Figure 4.19 Energy Release Rate, G vs. No. of Iterations

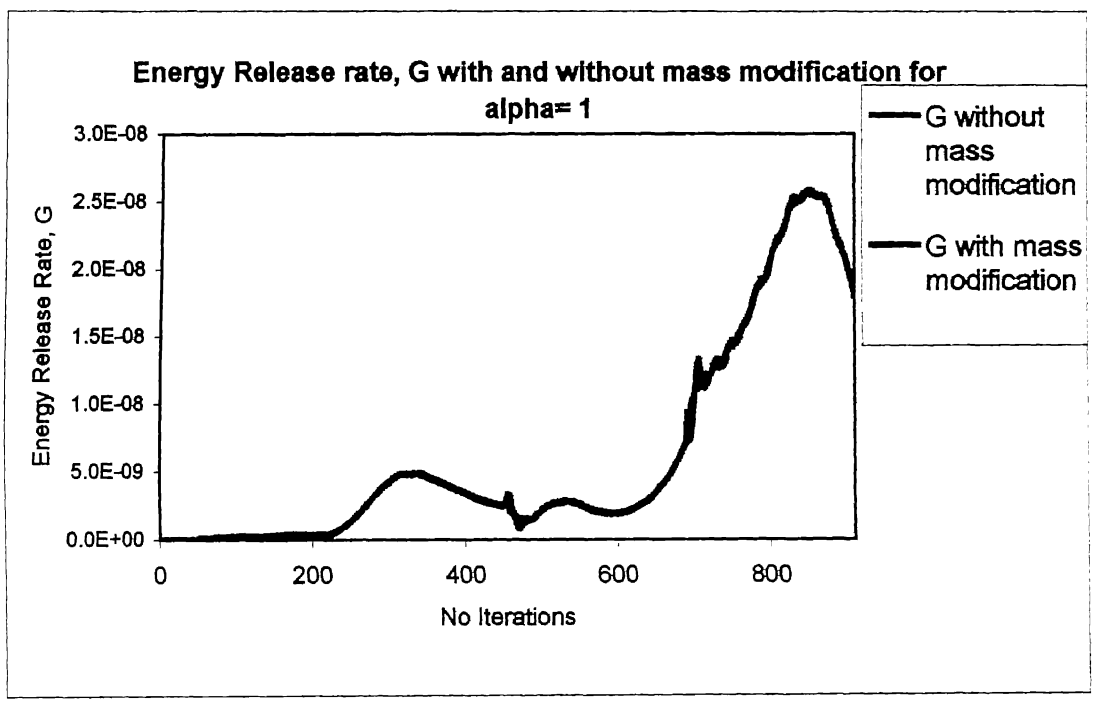

Figure 4.20 Energy Release Rate, G vs. No. of Iterations

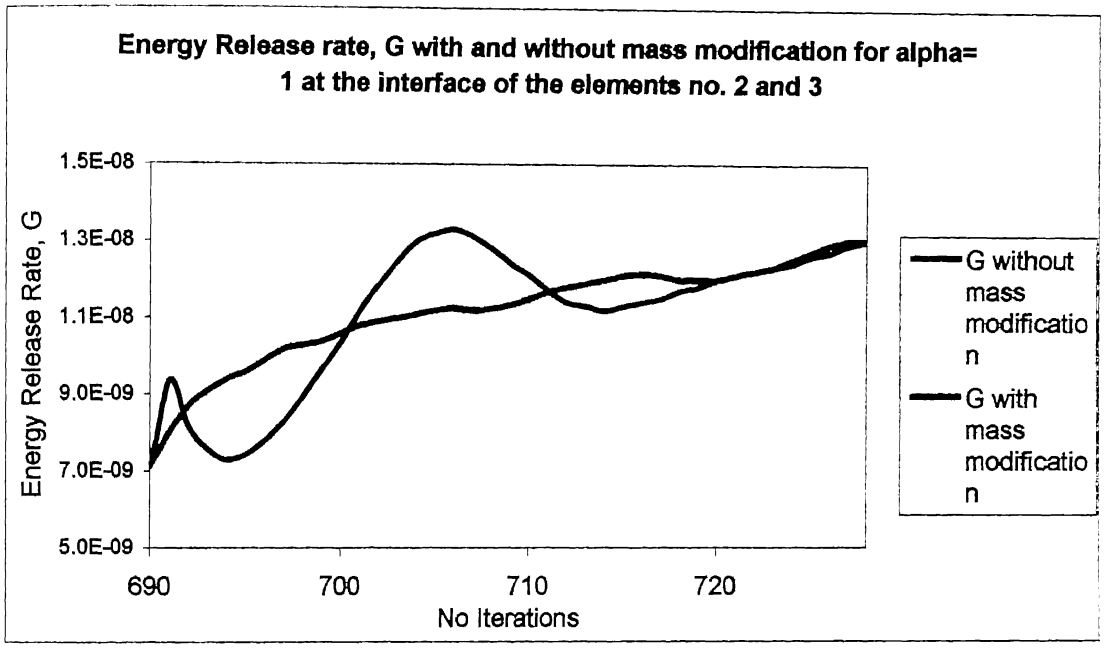

Figure 4.21 Energy Release Rate,G vs. No. of Iterations

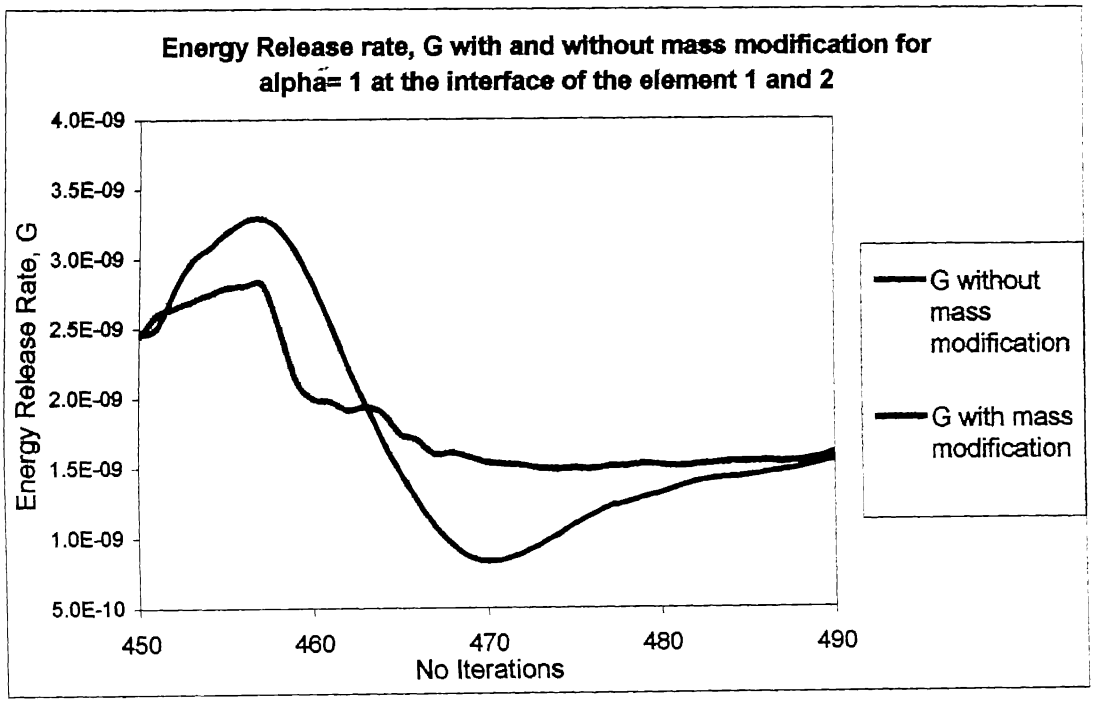

Figure 4.22 Energy Release Rate,G vs. No. of Iterations

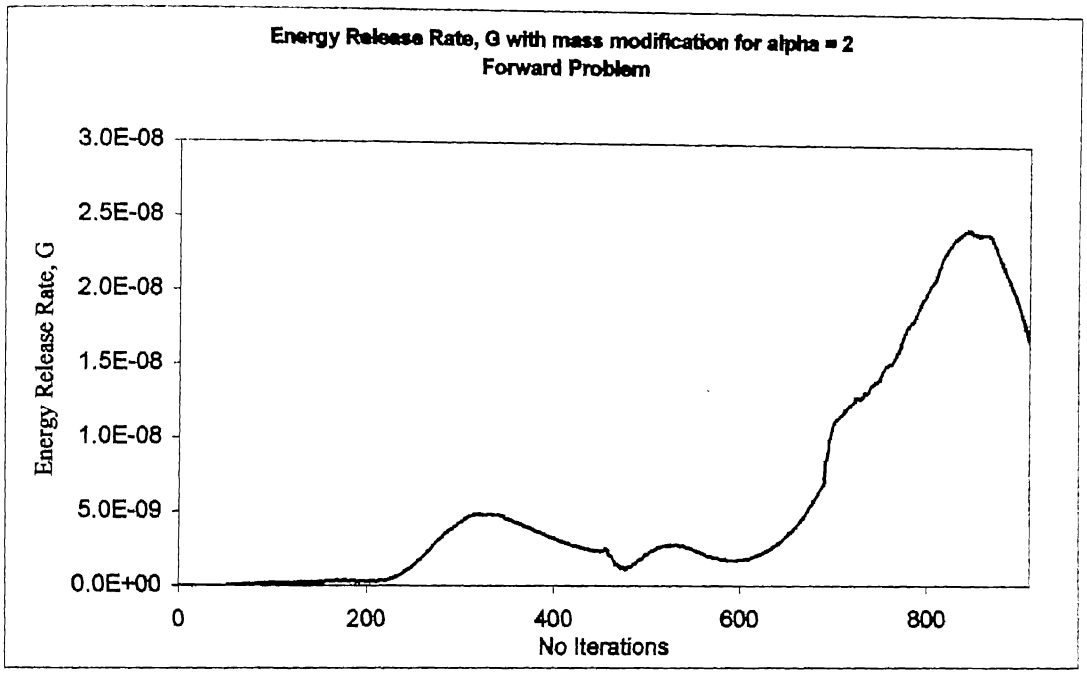

Figure 4.23 Energy Release Rate, G vs. No. of Iterations

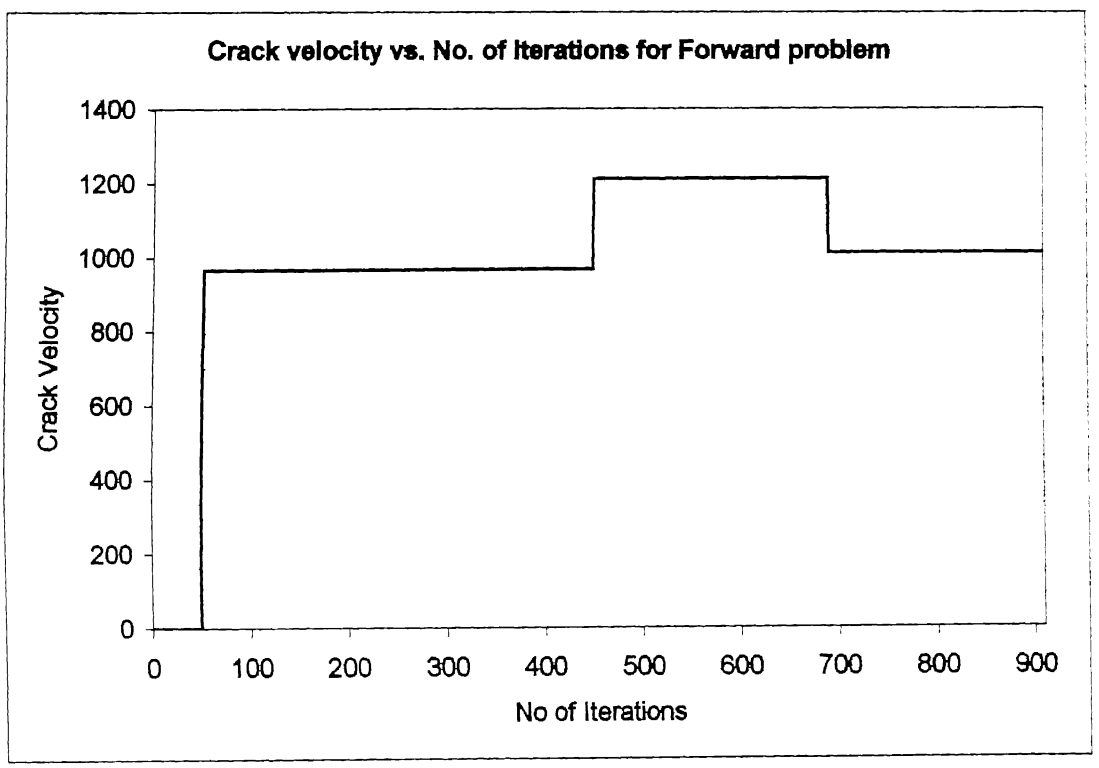

Figure 4.24 Crack Velocity vs. No. of Iterations

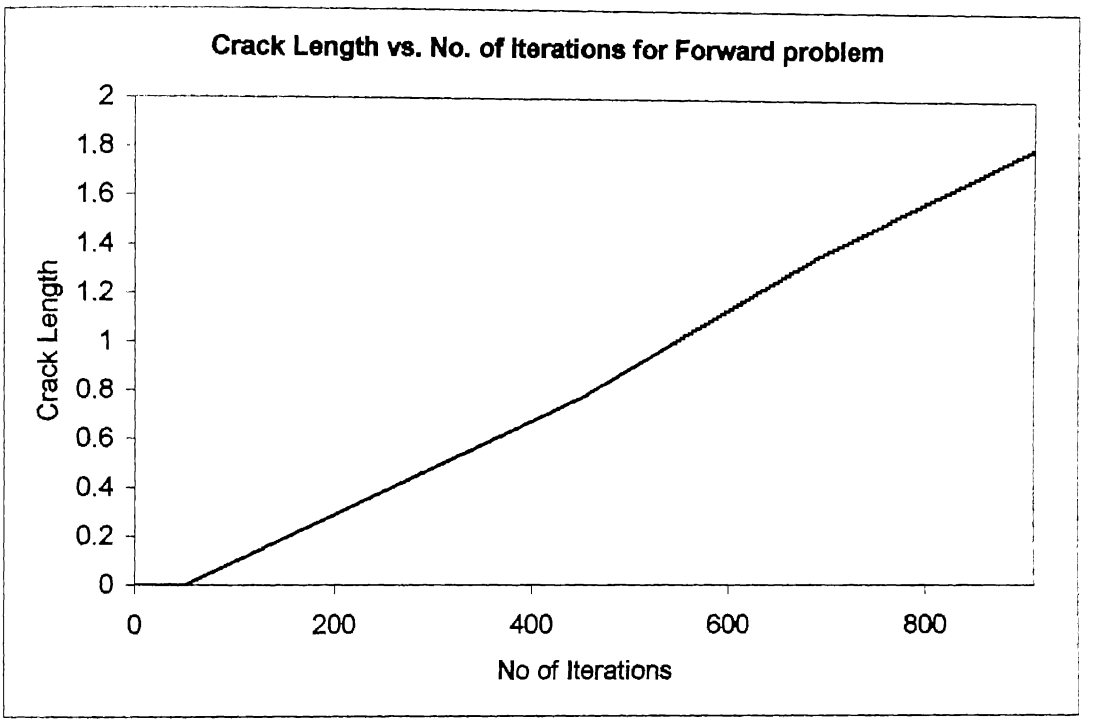

Figure 4.25 Crack Velocity vs. No of Iterations

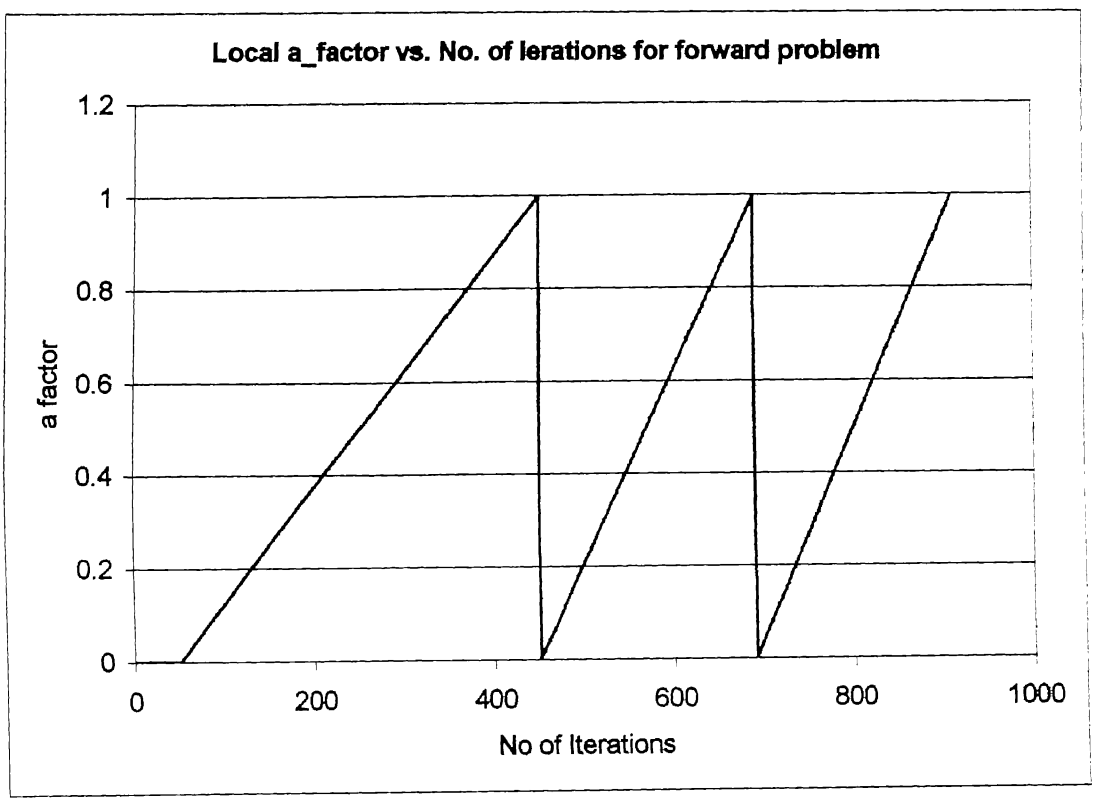

Figure 4.26 Local _a factor vs. No. of Iterations

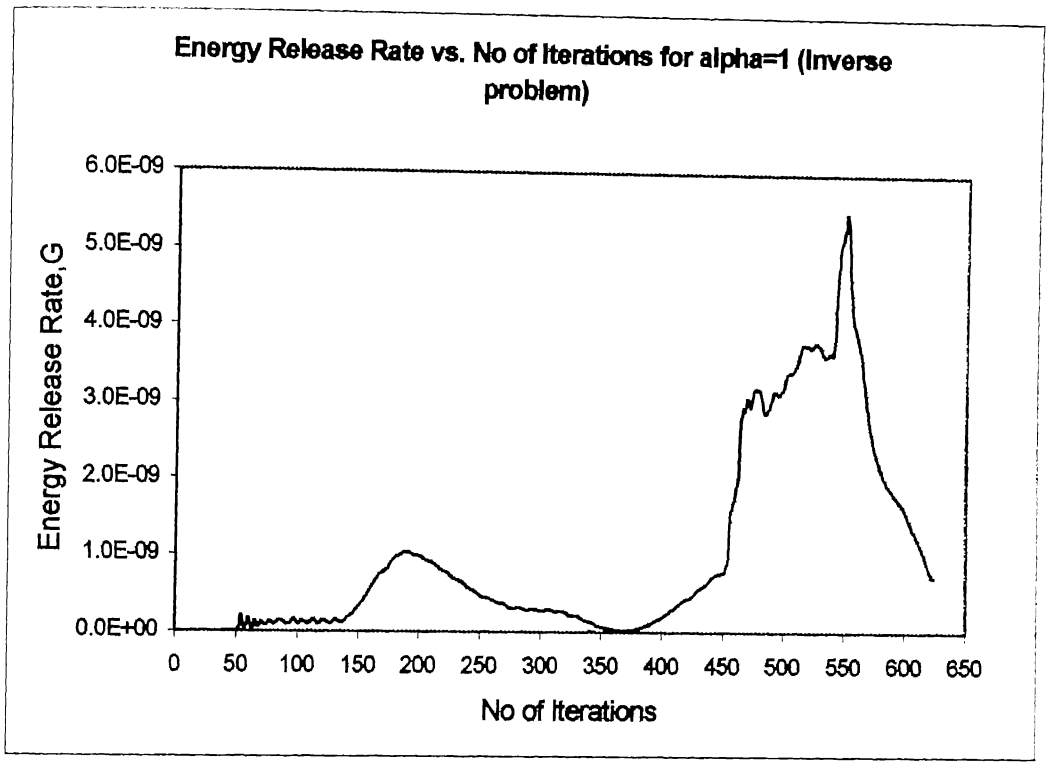

Figure 4.27 Energy Release Rate vs. No. of Iterations

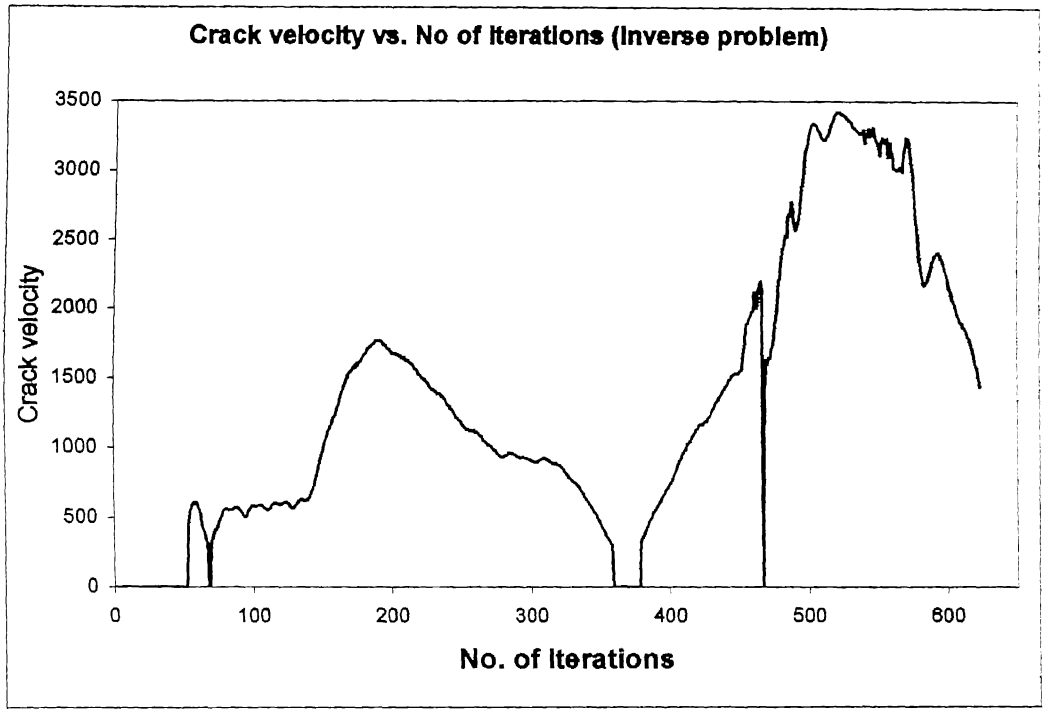

Figure 4.28 Crack Velocity vs. No. of Iterations

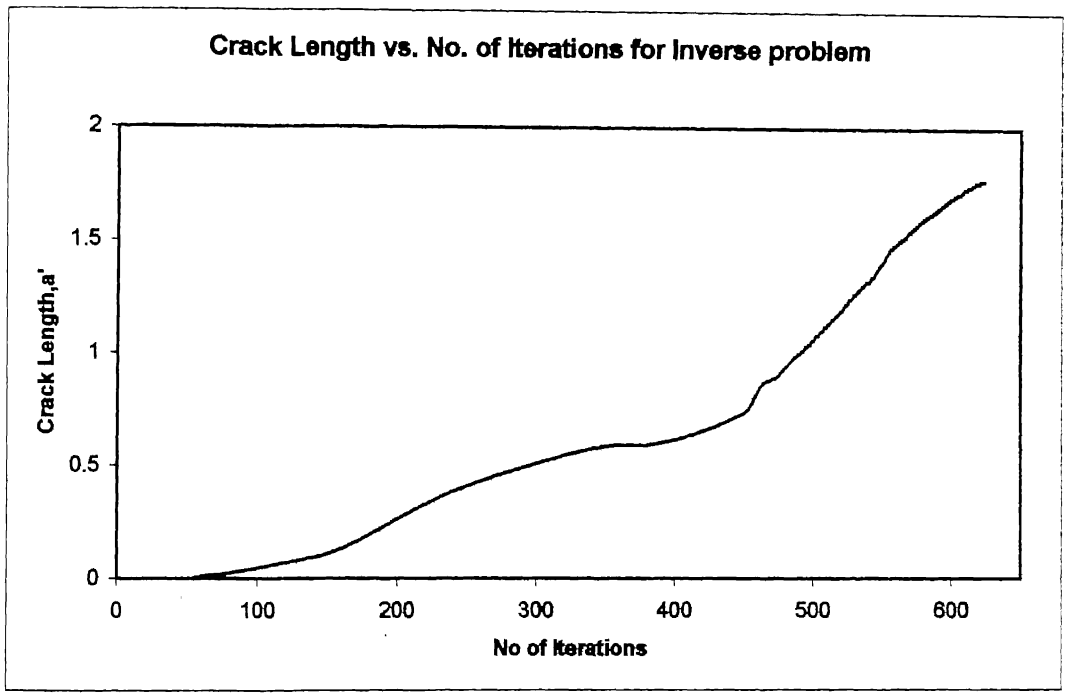

Figure 4.29 Crack Length vs. No. of Iterations

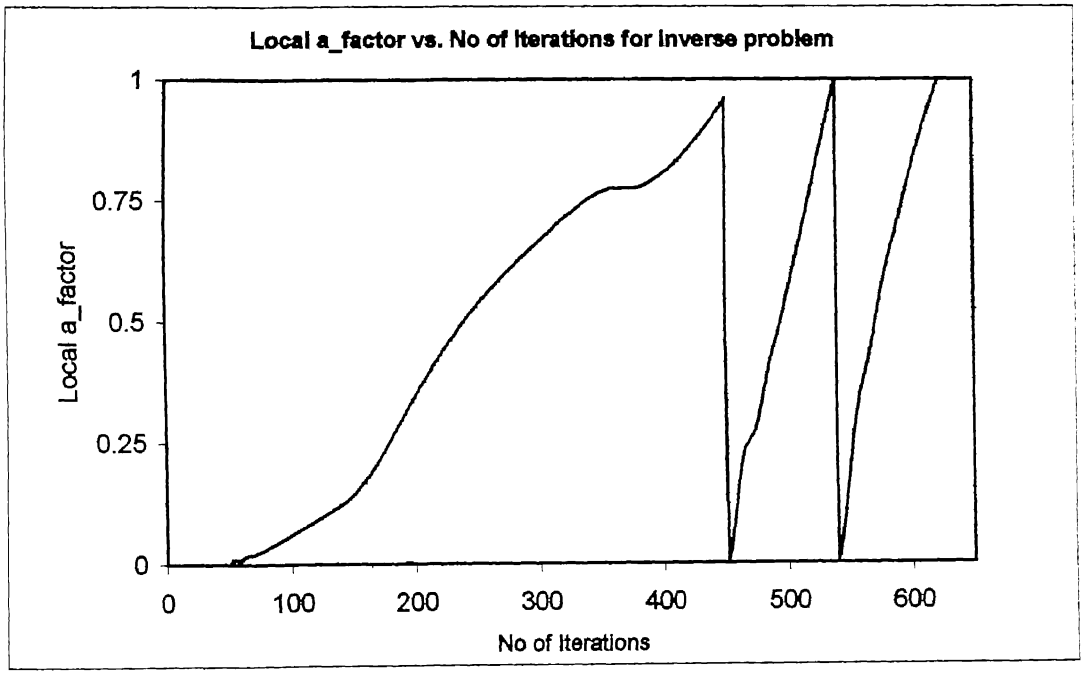

Figure 4.30 Local a _factor vs. No. of Iterations

CHAPTER 5

CONCLUSIONS AND SCOPE FOR FUTURE WORK

5.1 Conclusion

A modified stiffness release model is proposed to simulate high-speed crack propagation. This model is further improved for mass modification and based on the results and discussion in Chapter 4, following conclusions can be drawn.

1. Parameter α reduces dependence of the spring stiffness, K_s on C in stiffness release model.
2. For $\alpha>1$, the fluctuations in energy release rate at element boundaries is reduced.
3. Modified model gives fairly smooth and more stable variation of energy release rate.
4. Mass modification further reduces the fluctuations in energy release rate at the element boundaries

5.2 Scope for Future Work

1. The crack propagation model may be further improved to get still better results.
2. Present method can be extended to nonuniform crack speed.
3. This method can also be extended for 3-Dimensional crack propagation problems.

CHAPTER 5

CONCLUSIONS AND SCOPE FOR FUTURE WORK

5.1 Conclusion

A modified stiffness release model is proposed to simulate high-speed crack propagation. This model is further improved for mass modification and based on the results and discussion in Chapter 4, following conclusions can be drawn.

1. Parameter α reduces dependence of the spring stiffness, K_s on C in stiffness release model.
2. For $\alpha>1$, the fluctuations in energy release rate at element boundaries is reduced.
3. Modified model gives fairly smooth and more stable variation of energy release rate.
4. Mass modification further reduces the fluctuations in energy release rate at the element boundaries

5.2 Scope for Future Work

1. The crack propagation model may be further improved to get still better results.
2. Present method can be extended to nonuniform crack speed.
3. This method can also be extended for 3-Dimensional crack propagation problems.

References

[1] Nishioka T. and Atluri Satya N. (1986) Computational Methods in Mechanics of Fracture,ed. S.N. Atluri, Elsevier Science Publisher, New York

[2] Freund L.B., 1990, Dynamic Fracture Mechanics, Cambridge University Press, Newyork.

[3] Griffith, A.A. (1920),The phenomenon of rapture and flow in solods philosophical transaction of the Royal society (London)A221, pp.163-198.

[4] Owen D.J.R. and Shantaram D. (1977) Numerical study of dynamic crack growth by the Finite element method, International Journal of Fracture, Vol.13, pp. 821-837.

[5] Nishioka T. and Atluri S.N. (1982b) Finite element simulation of fast fracture in steel DCB specimen, Engineering Fracture Mechanics, Vol.16, pp.157-175.

[6] Nishioka T. and Atluri S.N. (1982a) Numerical analysis of dynamic crack propagation: Generation and prediction studies, Engineering Fracture Mechanics, Vol.16, pp.303-332.

[7] Chaing C.R., 1990, Determination of the Dynamic Stress Intensity Factor of a Moving Crack by Numerical Method, International Journal of Fracture, Vol.45, pp. 123-130.

[8] Thesken J.C and Gudmundson Peter (1991) Application of a moving variable order singular element to dynamic fracture mechanics, International Journal of Fracture, Vol. 52, and pp. 47-65.

[9] Kennedy T .C.and Kim J. B.,Dynamic analysis of cracks in micropolar elastic materials, Engg Fracture Mechanics, Vol. 27, pp. 227-298.

[10] Wang Y. and Williams J.G. (1994) A numerical study of dynamic crack growth in isotropic DCB specimens, Composites, Vol. 25, pp. 323-331.

[11] Chandra D. and T. Krauthammer, 1995,Dynamic effects on fracture mechanics of cracked solid} Engineering Fracture Mechanics Vol. 51, pp. 809-822.

[12] Kwang-Ho Lee, Jai-sug H. and Sun-Ho Choi, 1996, Dynamic stress intensity factors K_I, K_{II} and dynamic crack propagation characteristics of orthotropic material. Engineering Fracture Mechanics Vol. 53, pp. 119-140.

[13] Lin X. B. and Smith R. A., 1997,Improved numerical technique for simulating the growth of a planer fatigue crack. Fatigue and Fracture of Engineering Materials and Structures Vol.20, pp. 1363-1373.

[14] Beissel S. R., Johnson G. R. and Popelar C. H., 1998, An element failure algorithm for dynamic crack propagation in general direction. Engineering Fracture Mechanics Vol.61, pp.407-425.

[15] Zhuo Zhuang and Yongiin Guo, 1999, Analysis of dynamic fracture mechanisms in gas pipelines. Engineering Fracture Mechanics Vol. 64, pp. 271-289.

[16] Christina Bjerken and Christer Persson, 2001, A numerical method for calculation stress intensity factors for interface cracks in bimaterials}. Engineering Fracture Mechanics Vol.68, pp. 235-246

[17] Michael L. Falk, Alan Needleman, James R. Rice,2001, A critical evaluation of dynamic fracture simulations using cohesive surfaces ,Jounal De Physique IV.

[18] Efim A. Brener and Robert Spatschek, 2002, Fast crack propagation by surface diffusion, IFF, Jiilich, Germany.

[19] Siva Reddy, 1997, An FE model to investigate high-speed crack propagation. MTech thesis, Mechanical Engineering, IIT Kanpur.

[20] Girish V Deshmukh, 2000, A dynamic finite element model for high speed crack propagation analysis. M Tech thesis, Mech Engineering, IIT Kanpur.

[21] Mindlin,R.D.,1951,Influence of the rotary inertia and shear on flexural motion of isotropic elastic plates, J. Appl. Mech.,pp. 18-31.

[22] Zienkiewicz, O.C. and Taylor,R. L., 1991,The finite element method, fourth edition, Vol.2, McGraw Hill Book Company.

[23] Timoshenko, S. and Woinowsky-Krieger, S., 1959, Theory of plates and shells, McGraw Hill Book Company Inc.

[24] Bathe Klauss-jurgen (1990) Finite Element Procedure in Engineering Analysis, Prentice Hall of India.

[25] Keegstra P. N. R., 1976, A transient finite element crack propagation model for nuclear pressure vessel steels. J. Inst. Nucl.Engrs. Vol.17, pp. 89-96.

[26] Keegstra P. N. R., Head J. L. and Turner C. E., 1978, A two dimensional dynamic linear elastic finite element program for the analysis of unstable crack propagation and arrest. Numerical methods in Fracture Mechanics, Eds, A. R. Luxmoore and D. R. J. Owen (Univ. College Swansea), pp. 634-647.

[27] Malluck J. F. and King W. W., 1978, Fast fracture simulated by finite element analysis which accounts for crack-tip energy dissipation. Numerical Methods in Fracture Mechanics, Eds. A. R. Luxmoore and D. J. Owen (Univ. College, Swansea), pp. 648-659.

[28] Rydholm G., Freriksson B. and Nilson, 1978, Numerical investigation of rapid crack propagation. Numerical methods in fracture mechanics, Eds. A. R. Luxumoore and D. J. Owen (Univ. College, Swansea), pp. 660-672.

[29] Kobayashi A. S., Mall S., URABE Y. and Emery A. F., 1978, A numerical dynamic fracture analysis of three wedge-loaded DCB specimens. Numerical Methods in Fracture Mechanics, Eds. A. R. Luxmoore and D. J. Owen (Univ. College, Swanesa), pp. 673-684.

[30] Kishore N. N., Kumar Prashant and Verma S.K., (1993) Numerical Method in Dynamic Fracture, Journal of Aeronautical Society of India, Vol. 45, No.4, pp. 323-333.

[31] Aberson J. A., Anderson J. M. and King W. W., 1977, Dynamic analysis of cracked structures using singularity finite elements, in Elastodynamic crack problems. Ed G. C. Sih (Noordhoff, Leyden), pp. 249-294.

[32] Aberson J. A., Anderson J. M. and King W. W., 1977, Singularity-element simulation of crack propagation, fast fracture and crack arrest. Eds G. T. Hahn and M. F. Kannien. ASTM STP 627 ,pp. 123-134.

[33] Williams M. L., 1957, On stress distribution at the base of a singularity crack. Journal of Applied Mechanics,Vol. 24, pp. 109-114.

[34] Patterson C. and Oidale M., Analysis of an unstable crack growth and arrest problem using finite elements, Stability Problems in engg structures and

components, Eds T H Richards and P Stanley (Applies science publishers), 1979, pp. 281-296.

[35] Patterson C. and Oldale M.C., An analysis of fast fracture and arrest in DCB specimen using crack tip elements, Advances in fracture research, 1981, 5,ICF5, pp. 2225-2232